CHAPTER 1

INTRODUCTION

1.1 BACKGROUND OF STUDY

Chronic Obstructive Pulmonary Disease (COPD) is a disease which narrows the airway to the lungs progressively. The narrowing is mainly caused by the inflammation and thickening of the bronchi wall. As a result, airflow to and from the lungs are impeded. Thus, the symptoms that follow are shortness of breath, chest tightness, wheezing, chronic cough and sputum production. Cigarette smoking, exposure to air pollution, chemical fumes and dust further aggravates this progressive disease. National Heart, Lung and Blood Institute has recorded over 12 million people who are diagnosed with COPD who have yet to obtain treatments due to the minimal level of awareness regarding the disease. COPD was ranked sixth leading cause of death in 1990 and has been projected to become fourth leading cause of death worldwide by 2030 (Xiole Chen et al., 2011). Symptoms often worsen over time and can limit a patient’s ability to do routine activities. Gradually, simple everyday task such as walking, talking, and chores becomes a challenge and are subsequently inhibited in patient’s suffering with severe COPD. In most cases, COPD is diagnosed in middle-aged or older adults. Researches have yet to discover cures to reverse the damage to the airways and lungs. However, treatments and lifestyle changes can help a patient feel better, stay more active, and slow the progress of the disease.

Researches have taken various approaches to evaluate and treat this disease. However, the number of patients suffering from COPD is still recorded to be high in average (NH Johari et al 2010) primarily due to the failure to detect the symptoms of COPD at an early stage. Most times, these symptoms are misunderstood for other diseases. Therefore, this problem can be resolved by understanding the behaviour of airflow in the lungs during breathing. Equipped with better knowledge of the airflow mechanism in the lungs, medical officers could prevent the severity of this disease.

There are many scholars in the field did a researches on the behaviour of air and solid flow through the airway. But however there are not many researchers studied on the behaviour of air/solid flow on obstructed airway. Particle deposition is vital importance during these investigations. These airway regions are where the inhaled particles deposited with toxic chemicals and microorganism are liable to inflame or swell (Ulvestad et al., 2001). Meanwhile, it is also a parameter that could possibly be obtained by chemical or imaging method especially for the lower airway whose diameter could be too small to measure the flow pattern or velocity profile. From the medical treatment perspective, understanding of the relation between flow pattern and particle deposition would benefit the oral or nasal drug delivery device design which may facilitate high drug-aerosol deposition in desired pulmonary regions and reduce side effects. Early studies of airflow in the lung airways include the experimental work by (Proetz and Schroter and Sudlow 2004). A few velocity profiles and flow patterns were presented for a double bifurcation model. In other experimental studies the central airway up to the third generation of the bifurcation was used.

In this study, Computational Fluid Dynamics (CFD) was being used to simulate the airflow of model. CFD has certainly come of decades in field of applications and academic research. In early times, CFD was only limited to high technology engineering area such as aeronautics and astronautics, but now it is widely used in many field for solving complex problems which are derived from different discipline of fluid mechanics and heat transfer. Most of the researcher in this field is relying on this simulations tool to predict the airflow in the lungs as it is very difficult to obtain using experimental studies. The capability of this simulation tool is proven to give a good approximation results (NH Johari et al., 2010*)*.

A simplified model based on fifth to eighth generation human airway according to Weibel's 23-generation pulmonary model with a 70° bifurcation angle. The constrictions were place at different generation in the 4 generation airway model. Many researchers used Weibel’s 23 generation model as their research model because the symmetrical geometry and not to lose generality (H.Y Luo et al., 2007), (Arpad Farkas et al., 2007) (Xiaole Chen et al., 2009). The obstructed model is being modified from the reference model.

1.2 PROBLEM STATEMENT

Most of the early studies discuss about the symmetrical and asymmetrical airways and particle deposition (Maria Chiara Piglione et al., 2011), (Y.Liu et al., 2003), (Z.Zhang et al., 2004) and (X.Y Luo et al., 2004). They studied on the effect of bifurcation towards the airflow and particle depositions. The studies only analyse a smooth airway and the obstructed airways were ignored. Only a few did a research on obstructed airways (X.L Yang et al., 2005),(H.Y Luo et al., 2007) and (Xiole Chen et al., 2011). According to the studies, obstructed airway could alter the human airflow behaviour.

1.3 OBJECTIVE

Objective of the research are:

i. To determine the behaviour of the flow parameters through human airway with the presence of Chronic Obstructive Pulmonary Disease.
ii. To investigate the effect of different breathing mode on obstructed airway models

CHAPTER 2

LITERATURE REVIEW

2.1 INTRODUCTION

This chapter presents the structure and construction of bronchi, previous studies on the airflow in human lungs, and the behaviour of Chronic Obstructive Pulmonary Disease on the human airflow. Besides that the effect of obstructed airway location in the branches of the bronchi will be review.

2.2 HUMAN AIRWAY

The anatomy of human airway consists of trachea and complex branching tubes. The trachea has an inner diameter approximately around 2.5 centimetres and length around 10 to 12 centimetres for Asian. The trachea consist of lower border larynx and level with the sixth cervical vertebra. After that the trachea will bifurcate into two main branches, which are the primary bronchus then each of the bronchus will subdivide into smaller airway. A human respiratory may consist up to 28 generations of bronchi. One of popular lung model "Weibel model" by (Weibel .1963) had described a symmetrical tree structure of bifurcation bronchi with 23 generation. The function of trachea and bronchi is to transport air from mouth to alveoli or vice versa. Trachea and bronchi are important organs in human body as any damage happen on it could affect or change the behaviour of human airflow.

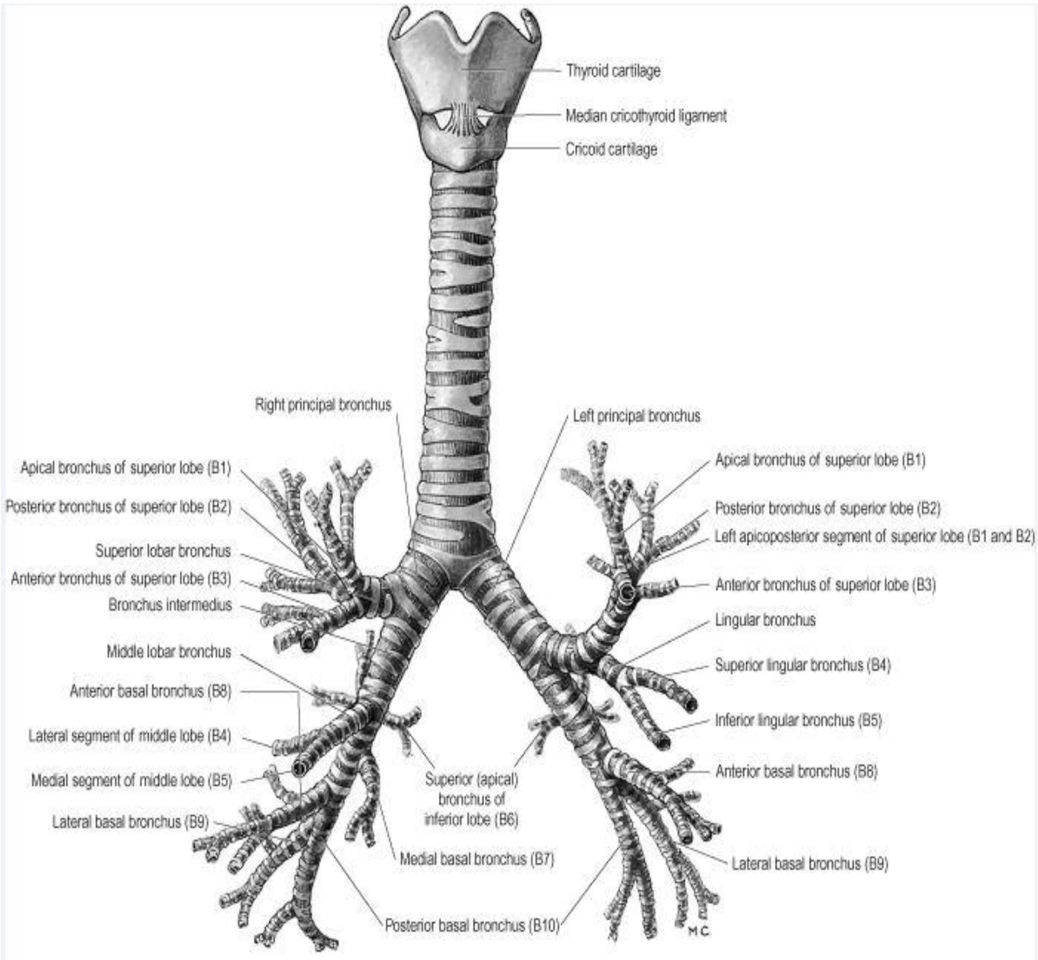

Figure 2.1 : Trachea, and bronchi.

Source :(Drake R, Vogl AW, Mitchell AWM, et al: Grays Atlas of Anatomy. Philadelphia, Churchill Livingstone/Elsevier, 2008)

2.3 SIMPLIFIED AIRWAY

A normal simplified airway model is combinations of cylinders, which are define by length and diameter only. The curvature, surface irregularities, asymmetrical properties are neglected in this case. One of the earliest simplified models constructed are "weibel model" the 23 generations of trachea and bronchi (Weibel 1963), (Horsfield et al., 1971), (Schlesinger and lippman 1972). Although the simplified model would be differing from a realistic model, many researchers did studies on the simplified model, to accelerate the time and discuss on other issue such as the effect of velocity and pressure rather than the model.

2.4 AIRFLOW IN SYMPLIFIED MODEL

Most of the researcher in previous studies used a simplified airway models to study the airflow behaviour in the lungs. (Y.liu et al., 2002) studied about the bifurcating airflow in human lung airway. According to (Y.Liu et al., 2002), human lung tubes are elastics and able to move because the interaction between lung tube and fluids. But in his studies, the lung tubes are considered to be rigid, as the study will only focus on flow part. In his research, he used weibel model (1963) from 5^{th} generation to 7^{th} generation and modified to in plane and 90 degree off plane. He studied the effect of in plane and off plane to the airflow in the lungs. A two generation of airway model may not produce a realistic figure of flow field in respiratory airways as the bifurcation in respiratory model would give disturbances, which affect the air flow behaviour in subsequent generation-bifurcating airway. (Y.liu et al., 2003) also did a research on the effect of asymmetrical airway to the airflow based on Weibel model. The use of double bifurcations as in symmetric lung model as the addition of more branches would increase the computation. But, using a triple bifurcations require more cells and the running time would increase. A three generation of airway model is been used as there is no experimental data available for four generation airway models in the open literature.

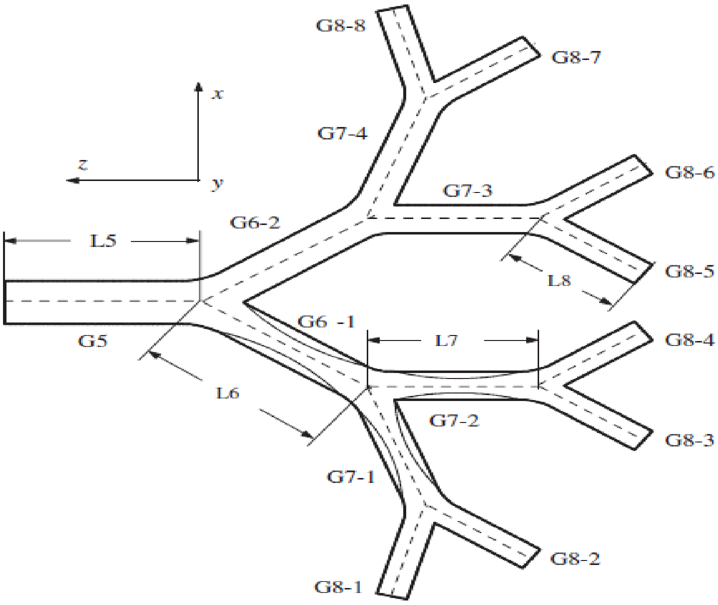

Figure 2.2: Simplified model using dimension from Weibel (1963). Two dimensional model.

Source:X.L Yang et al., 2006

2.5 OBSTRUCTED AIRWAY DISEASE

Obstructed airway disease is group of conditions which distinguished by the resistance and obstruction in the air passages. Obstructed airway disease includes bronchial asthma, chronic obstructive pulmonary disease (COPD), and the common cold. The basic causes of obstructive airway disease are cigarette smoking, infections and dust allergies.

2.5.1 Asthma

Asthma is an obstructive airway disease where the tubes of bronchi are extra sensitive. The airway becomes inflamed and produces mucus. The muscles around the airways becomes tight and making the airways narrower. Asthma is usually caused by breathing in particles such as dust or pollen that produce an allergic reaction. Other than that, it can be triggered by upper respiratory tract infection, cold air, exercise or smoke. Asthma affected more than 300 million people around the world and it is consider a common condition. Asthma may cause wheezing, breathlessness, chest tightness, and coughing particularly in the early morning.

- **Exercise-Induced Asthma** — is a common asthmatic problem mainly happen after involves in outdoor activities such exercising in a cold weather.
- **Occupational Asthma** — an estimated 2% to 5% of all asthma episodes may be caused by exposure to a specific sensitizing agent in the workplace.
- **Nocturnal Asthma** — is a characteristic problem in poorly controlled asthma and is reported by more than two thirds of sub-optimally treated patients.

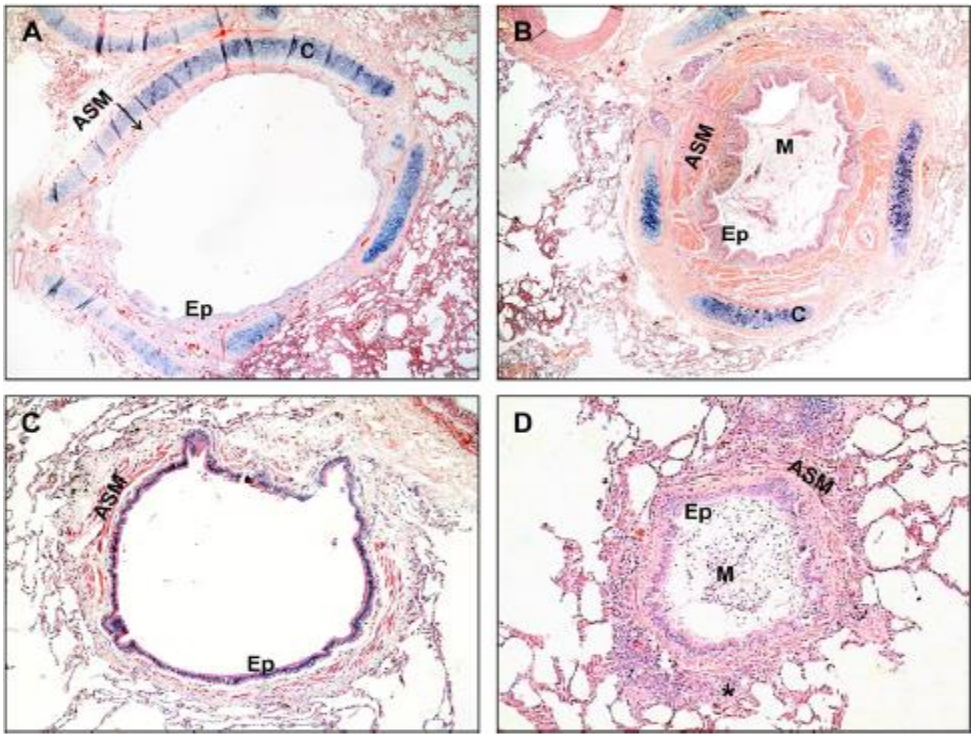

Fig 2.3: A and C, Normal airways. B and D, Airways from a patient with fatal asthma. Mucus plug within the airway lumen, epithelial folding and thickened ASM layer in B. Mucus plugging and increased ASM thickness in D, with spreading of the inflammation to the surrounding per bronchiolar alveoli.* Haematoxylin and eosin. A and B, 325. C and D, 3100. C, Cartilage; Ep, epithelium; M, mucus.

Source: Joshua A. Boyce et al., 2007

2.5.2 Bronchiectasis

Bronchiectasis is an abnormal, irreversible dilatation of the bronchi which are caused by destructive and inflammatory changes in the airway walls. There are three major anatomical patterns of bronchiectasis which are cylindrical bronchiectasis, varicose bronchiectasis and cystic bronchiectasis. Bronchiectasis will alter the airflow by damaging the airway to widen and become flabby and scarred. The airways are the bronchi tube that carries airs throughout the lungs. Bronchiectasis mainly caused by infection and other condition which injured the walls of the airways or to prevent the airways from clearing the mucus. Mucus is a slimy substance which helps to remove inhaled dust , bacteria, and other small particles from the airways. In bronchiectasis, the airways will lose the ability to clear out the mucus. Hence, the bacteria will grow up as the mucus builds up. This will lead to serious lung infection and each infection causes more damage to the airways. Over the time, the airflow movement will be disturbed as the airway can't properly move air in and out. This will results the not much oxygen will pass through the alveoli.

Fig 2.4: Cylindrical bronchiectasis.

Source: Michael Baydarian et al., 2008

2.5.3 Chronic obstructive pulmonary disease (COPD)

Chronic Obstructive Pulmonary disease is considerable morbidity and is predicted to become the third leading cause of death worldwide by 2020 (Murray CJ, Lopez AD 1997). Chronic obstructive pulmonary disease (COPD) is considered to happen in three related conditions which are bronchitis, chronic and emphysema. In each of the related condition there is chronic obstruction in the airway of the lungs and the obstruction are generally irreversible and maybe progressive over time. In chronic bronchitis, the airway of the bronchi is inflamed and makes a lot of mucus. The bronchi are happen to be obstructed which the airways that airs go through become narrower and the airflow becomes limited. In emphysema, the air sacs in the alveoli are damaged and lose the ability to stretch. Hence less air enters through the lungs , which makes feel shortness of breath. Chronic obstructive pulmonary disease (COPD), also known as chronic obstructive airways disease (COAD) or chronic airflow limitation(CAL). This group of disease is considered as airflow limitation which is not fully reversible. The airflow throughout the lungs is impaired. This disease can be measure using a peak flow meter and spirometry. The COPD conditions emphysema and chronic bronchitis although most patients have the both conditions to varying degree. While in asthma the obstruction airway is reversible and often considered separately, but many COPD patients have some certain of reversibility in their airways. In this disease, as increase in airway resistance, the force expiratory volume decreased in 1 second (FEV1) measured using spirometry. COPD is defined as a forced expiratory volume in 1 second to forced vital capacity ratio (FEV1/FVC) that is less than 0.7. Residual volume is often increased with COPD as the volume of air left in the lungs following full expiration. Hence it could result in the clinical feature if a “barrel chest” which means a chest with a large to back diameter. The most common cause of COP is cigarette smoking and breathing in other particles, and gases. It is progressive disease which develops after about 20 years of smoking. Hyperinflation can be checked through chest x ray, but the lung damage of COPD is not visible on a chest x ray. The damage of lung caused by COPD is visible in CT scan. COPD is generally irreversible, but the lung function can partially recover if the patient stop smoking. Severe emphysema has been treated with lung volume reduction surgery, with some success in carefully chosen cases. Lung transplantation is also performed for severe COPD in carefully chosen cases.

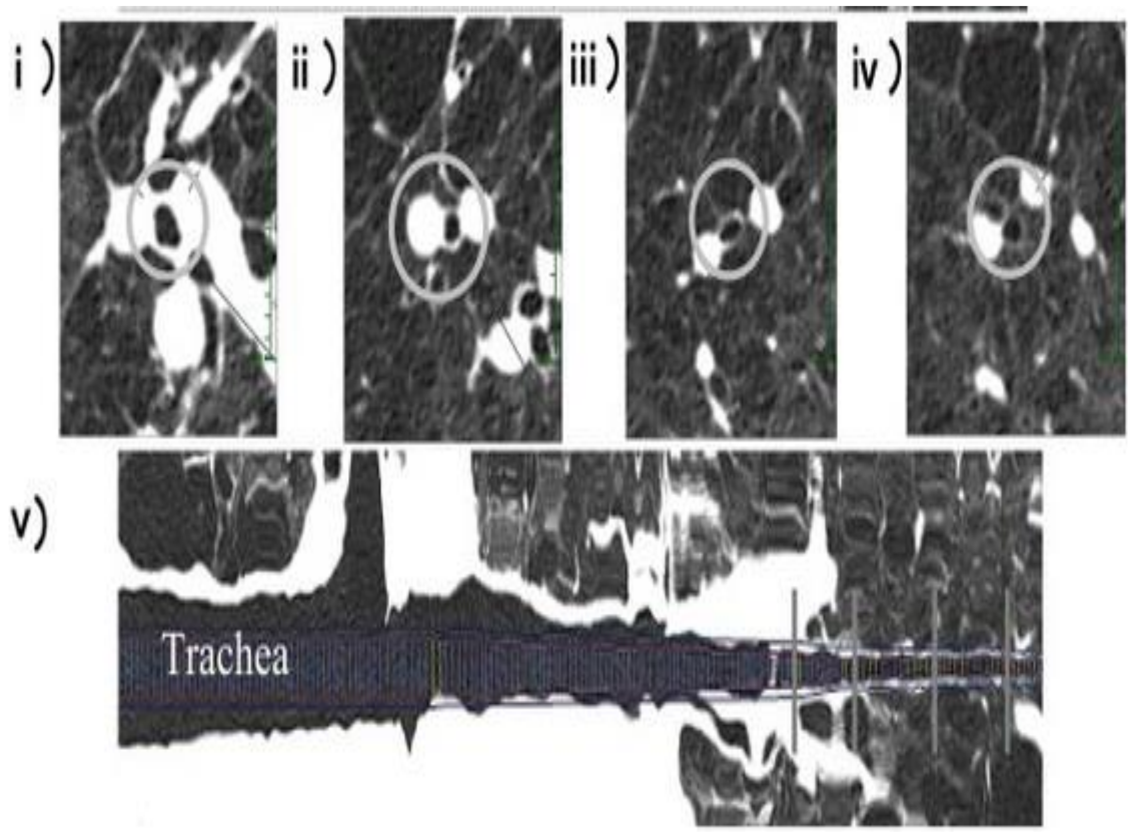

Fig 2.5: Images of a patient with COPD (FEV_1,%predicted 62.9%, FEV_1/FVC 49.8%) Short-axis image of the bronchus in i) the third generation ii) the fourth generation iii) the fifth generation iv) the sixth generation are shown. v) is the curved multiplanar reconstruction image and grey lines and circles indicate the same sites analysed. Short-axis images, obtained from a curved multiplanar reconstruction image, are precisely perpendicular to the long-axis of the airway. Identification of the generation of bronchi relied on careful inspection, simultaneously using longitudinal and short-axis images and searching for any bifurcations in the entire circumference.

Source: K. Shimizu et al.,2011

2.6 STUDIES ON OBSTRUCTED AIRWAYS

In obstructed airway studies, researcher had done studies about the obstructed airway in different sizes, locations and tumours in the simplified airway model. (X.L Yang et al., 2006) had done research on obstructed airflow in 4 generation airway model. The airway models are constructed based on 5^{th} to 8^{th}, 23^{rd} generations of weibel (1963). Hence to study the effect of obstructed flow, the simplified model are modified in 3 different model which the obstructed airway are place in different generations of the airway. The obstructed airways are considered to be contracted to half of the normal diameter. (H.Zhang et al., 2010) had discussed on the asthmatic airway which are modified from 10^{th} to 11^{th} generation of Weibel model. In this case the researcher didn't contract the obstructed airway into half of the normal diameter but implement a folding pattern to the obstructed airway. To create such a folding pattern in this work, the cross-section of the asthmatic airway is modelled as a circular area surrounded by a number of sinusoidal folds uniformly distributed along the circumference. (A. Farkas et al., 2007) had discuss the effect of obstruction and blockage on airflow and aerosol deposition in central human airways. (Farkas et al., 2007) also used weibel model 3^{rd} to 5^{th} generation. From the weibel model , the researcher modified to different unhealthy models e.g. tumorous models and blocked airway model.

a)

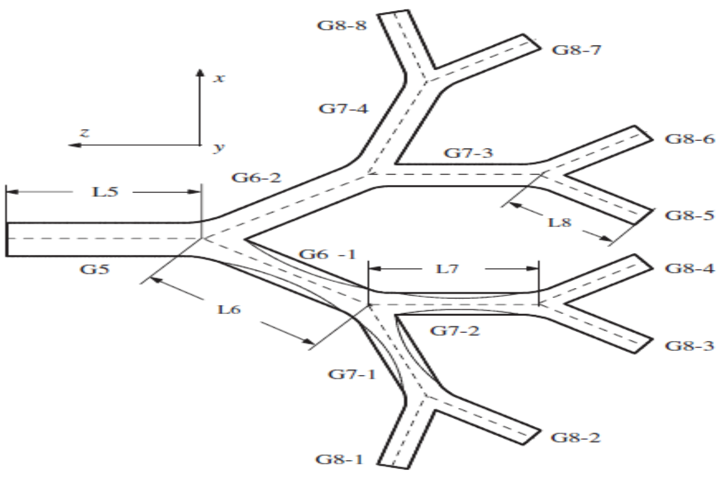

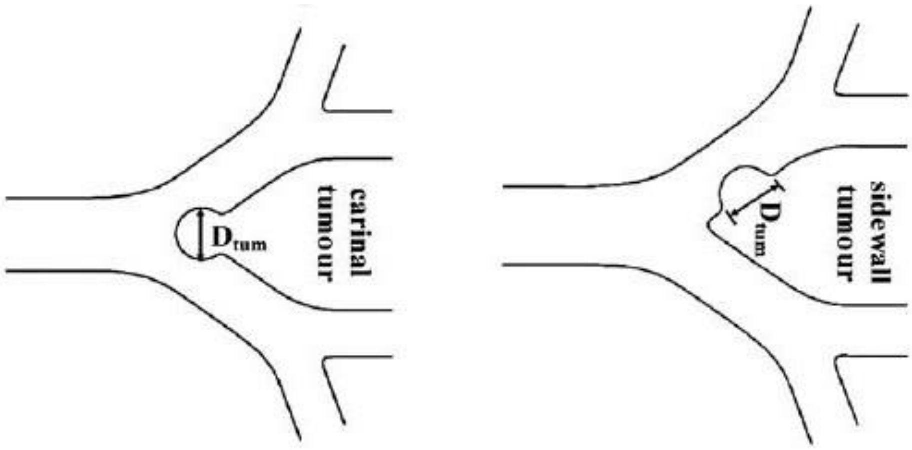

b)

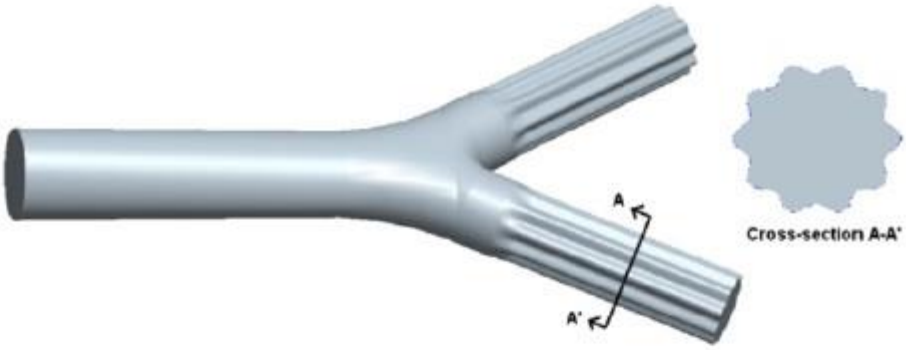

c)

Fig 2.6: view of simplified model of a) X.L Yang et al., 2006, b) A. Farkas et al., 2007, c) H.Zhang et al., 2010

2.7 ANALYSIS ON SIMPLIFIED AIRWAY MODEL

In a simplified airway model, the air flow pattern are impinges to the inner wall and then turns to move to outward along the top and bottom walls to merge at the outer wall of the tube. The flow from the top and bottom wall merges to form two counter-rotating vortices. This will cause the axial velocity profile to skew to the inner wall. In the third generation of airway the air flow in lateral branches are much weaker than the medial airway. This is because the skewed velocity towards the inner wall in the upper airway branches. Hence more air will enter the medial airways (Y.liu et al., 2003). In a lower Reynolds number, the secondary flow is weak to produce M shaped axial velocity profile in the transverse plane of the airway. However in a higher Reynolds number, the M shaped velocity profile in transverse plane is visible because effect of secondary flow due to bend curvature and the flow divider . With increase in Re; the axial velocity profile shifts from parabolic to M-shape, indicating a stronger secondary flow at higher Reynolds number (Y.liu et al., 2002).

a)

b)

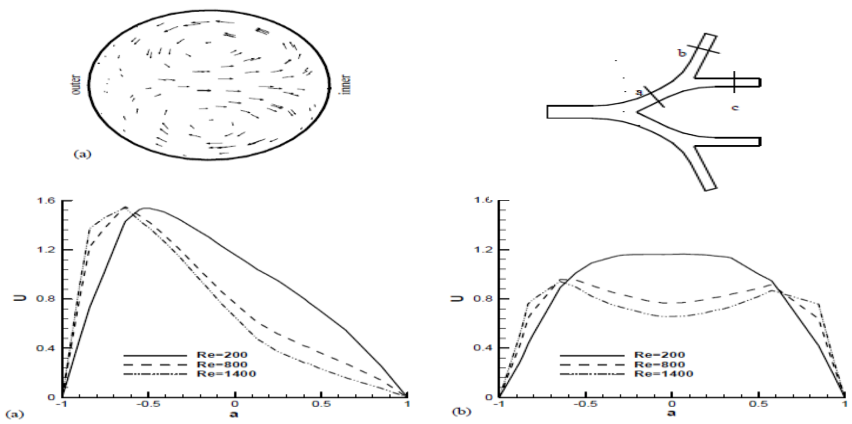

Fig 2.7 : a)Secondary flow vectors at cross sections of a three-generation airway: (a) the middle section of the second-generation branch. b) Axial velocity distributions the airway: at the middle of the in-plane second-generation branch in the bifurcation Plane and the middle of the in-plane second-generation branch in the transverse plane.

Source: Y.liu et al., 2002

For the in-plane bifurcation model, the bifurcation planes of the second and third generation airways are co-planar, and the velocity profile is skewed towards the inner wall at the second-generation airway. This behaviour leads to an imbalance in the flow partition throughout the medial and lateral branches. For a symmetric bifurcation, the secondary flow in the lateral branch is very weak. In this asymmetric model, due to the larger size of the lateral branches, most of the fluid has been attracted into the lateral tubes in the third bifurcation. Consequently, the secondary flow in the lateral branches of the third bifurcation has been enhanced significantly compare to the symmetric bifurcation. Pressure drop in the bifurcating airways plays an important role in the respiratory process. The respiratory process can only take place continually and normally when the alternative contraction and expansion of the respiratory muscles overcomes the pressure drop due to viscous and other losses.

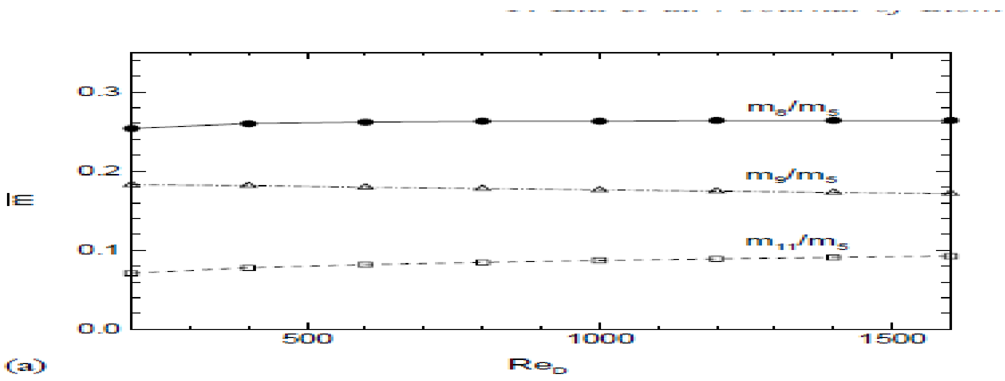

b)

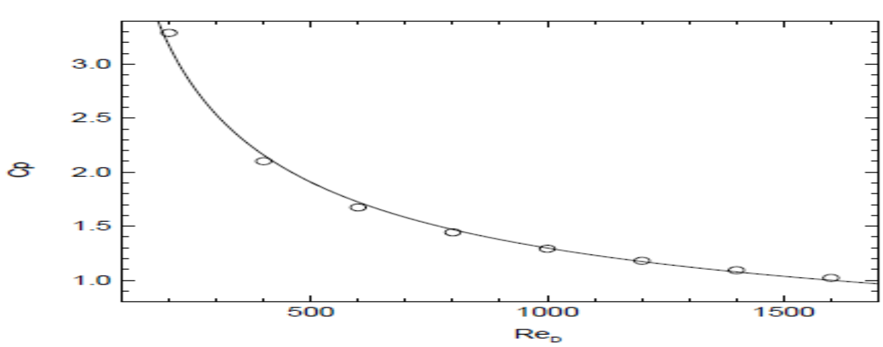

Fig2.8 : a) Variation of the mass flowrate ratio with ReD, Between the upper daughter branches and grandmother airway G5. b) Variation of the pressure drop coefficient Cp with ReD.

Source: Y. Liu et al.2003

2.8 ANALYSIS ON OBSTRUCTED AIRWAYS

In the previous studies, researcher had done research on the effect obstructed airway to the air flow and their finding are very beneficial to this present studies. According to them the obstructed airway will alternatively alter the behaviour of normal healthy airway model. The obstructed airway will create jet effect which would produce the highest velocity in the model. In the obstructed airway, a recirculation will happen which will block the air to enter the lower branches. According to (Arpad Farkas and Imre Balashazy, 2007) the airway narrowing accelerates the air, inducing high velocity values at the outlets. The outlet velocities in the non-occluded branches are also enhanced in the case of airway blockage. Airway blockage produced upstream effects as well. As a result of the blocked fifth-generation lateral branch the velocity gradients became lower at the outer side and higher at the inner side of the fourth-generation upstream branch.

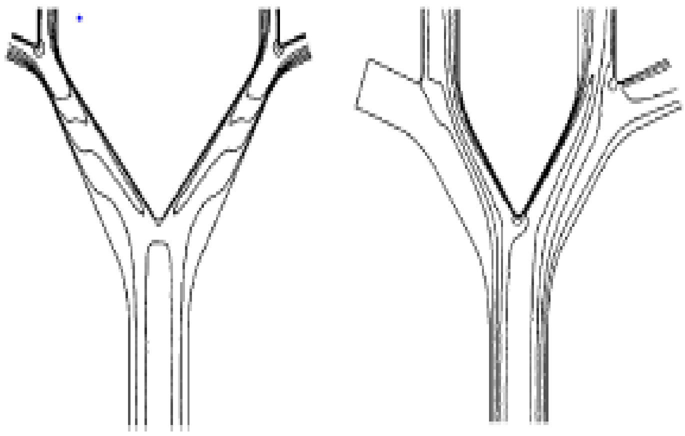

Fig 2.9: City isolines in case of narrowed airways; right panel: velocity isolines in case of bronchial airways with one of the fifth-generation lateral airways blocked.

Source: Á. Farkas, I. Balásházy. 2007

A parabolic velocity inlet profile in our symmetrical healthy airway model leads to equal flow rates in the fourth generation branches. However, an imbalance flow partitioning due to the skewed axial velocity in fourth-generation airways can be observed at the level of fifth-generation branches. As a result, in medial branches flows more air than in lateral daughters. The presence of airway disorders can induce further imbalances. (A. Farkas, I. Balásházy, 2007) had compared the computed flow rate weightings *(Wi)* in the case of the analysed diseased and healthy airways in the fifth-generation branches. The results demonstrate significant flow redistributions in case of sidewall tumours. The flow rates in the branches down to the tumour decrease (especially in the medial branch) with the increase of tumour diameter. In case of central tumours and bilateral narrowing, the flow is still symmetrically distributed, but the ratio of median to the lateral flow rates is smaller when compared to the case of healthy airways. In case of bilateral airway constriction the flow was almost equally distributed in the four branches. The flow rate in a completely blocked branch is obviously zero. In the studied case the flow proved to be weighted almost equally in the three non-occluded fifth-generation ducts when one of the lateral branches (out1) was blocked. If one of the medial branches (out2) or both the lateral and medial branches (out1 and out2) are blocked, then the flow rate increases in the non-occluded branches in a more accentuated way.

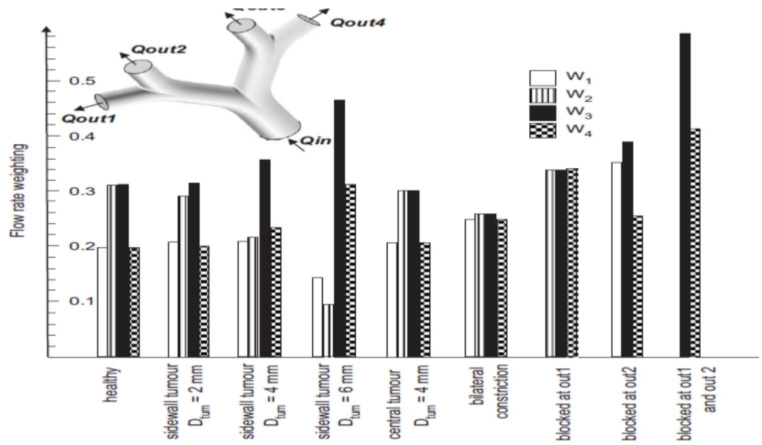

Fig 2.10 : Splitting of the inspiratory airflow at the outlets of healthy and diseased airways. *Q*in *(*=2.25 l/ min*)* is the inlet flow rate, *Q*out1, *Q*out2, *Q*out3, and *Q*out4 represent the outlet flow rates and *W*1, *W*2, *W*3 and *W*4 denote the flow rate weightings. *D*tum is the symbol for tumour diameter.

Source: Á. Farkas, I. Balásházy, 2007

2.9 PRESSURE DROP BEHAVIOR

The change of pressure in lung airways and alveoli is the driving force in the process of respiration. Therefore, it is necessary to understand the influence of the boundary condition on the pressure drop. The bar graph of *Cp* in different models with different inlet velocity boundary conditions is shown in Fig. 10. It can be clearly seen that in all models, the pressure drop coefficient *Cp* in the cases with uniform inlet velocity profile is much higher than those in the cases with other types of inlet velocity profiles. Nevertheless, the pressure drop coefficients *Cp* in the cases with parabolic, positive-skewed, and negative-skewed inlet velocity profiles are almost the same in each model. The pressure drop coefficient *Cp* in the case with uniform inlet velocity profile is about twice of those in the cases with other types of inlet velocity profiles. Consequently, the uniform inlet velocity profile may lead to inaccurate result of pressure drop.

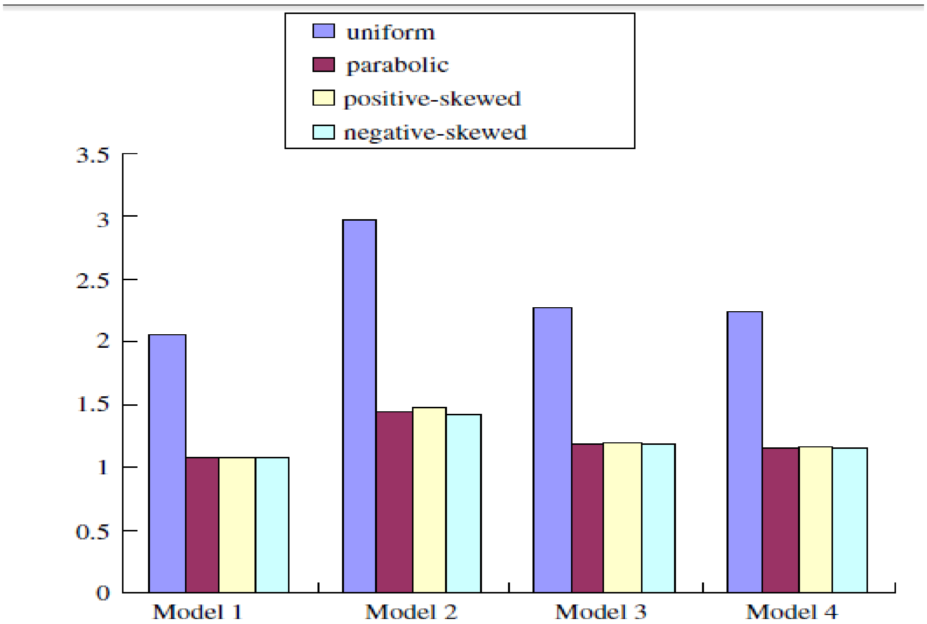

Fig 2.11: The pressure drop coefficient, *Cp*.

Source: X.L. Yang et al.2006

CHAPTER 3

METHODOLOGY

3.1 INTRODUCTION

The methods been used in achieving research's objective will be discussed in this chapter. This chapter describes the research design, research instrument and analysis as well. In methodology part, work flow and methods is discussed on how to complete the study. At the beginning, project was started by doing gannt chart. All the planning with the duration were clearly stated, and managed finish all the task by referring this chart. By the aid of supervisor, steps required to succeed this study is well understood. All the activities that required in this project were arranged sequent in flow chart. It is easier to refer flow chart while conducting research, because the steps are there and if stuck or data went wrong, there will be an alternate way to redo the experiment. By doing this, research time can be saved and do not have start from beginning but important steps cannot be skip. The rest of work flows were discussed further in following pages.

3.2 FLOW CHART

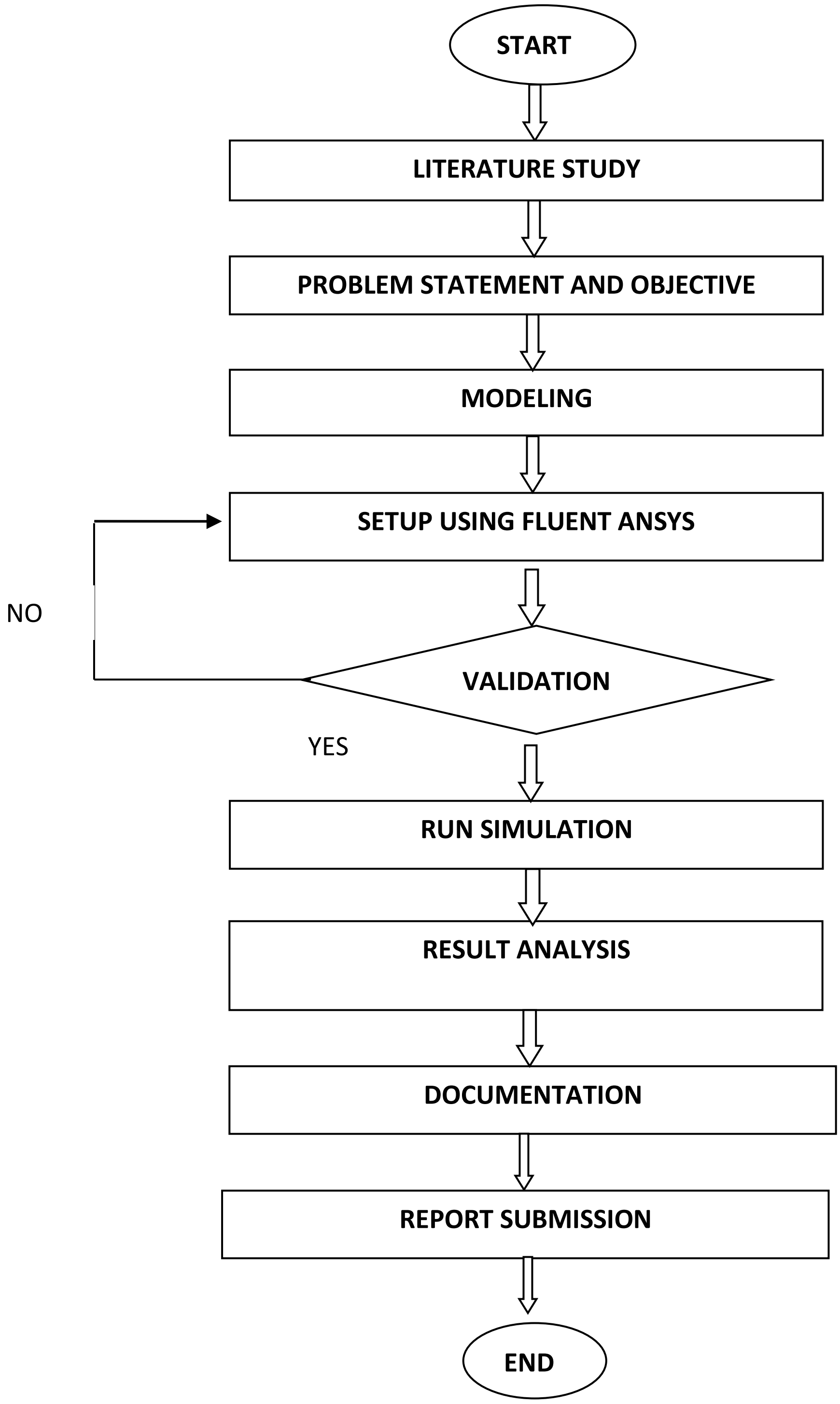

Figure 3.1: Process Flow Chart of Study

3.3 METHODS

In this project, Computational Fluid Dynamics (CFD) Fluent version 14.0 is used to run the simulation. A finite volume method is used to solve the Navier Stokes and continuity equation on the domain using boundary conditions. The model geometry is constructed using Solid work version 2010 using the appropriate parameters. The Parameters for the geometry are tabulated in the table 3.3. The convective terms are all discretized using second order upwind scheme and the SIMPLEC method is used for the pressure–velocity coupling. In addition, the pressure interpolation scheme is specified as second order. The multi grid method is invoked to increase the speed of convergence of numerical solutions. To ensure the solution accurate and stable, conservative under-relaxation factors are selected to be 0.3 for pressure and 0.5 for momentum. A parabolic velocity profile is imposed on the inlet; the static pressure is set to be zero at all outlets; no-slip wall boundary condition is imposed on all solid walls.

3.4 MODEL GEOMETRY

A schematic view of the model is been shown in fig.3.2. The symmetrical model is shown by the bold line. The model is constructed based on 5^{th} to 8^{th} generation model from weibel 23 (1964). The angle between each branch is 70 degree. The length and diameter of the model is equal to Weibel's model respectively. To study the obstructed airflow along the airway, the symmetrical model is modified. For model 2 the diameter of 6^{th} generation airway is contracted to half of its original size. For model 3 the diameter of the lateral 7^{th} generation airway is contracted to half of its original size and for model 4 the medial 7^{th} generation airway is contracted to its half of original size. Certain assumptions were also needed to create smooth bifurcations. Since the Weibel model only defines one diameter for each generation of airway, it would be natural to assume that each branch at a given generation has uniform diameter. However, this would lead to drastic discontinuities at the bifurcations. In order to eliminate these discontinuities, it was assumed that each daughter branch began its separation at the bifurcation point as the frustum of a cone.

The large diameter of the frustum was set equal to the diameter of the parent branch and the small diameter of the frustum equal to the daughter branch. The length of the frustum was set equal to one tenth of the length of the daughter branch. The resulting shape yielded a carinal ridge with a broader included angle than that expected from the union of two cylinders. (Comer et a.l,2005) have investigated the effect of rounding of this cardinal ridge, albeit for bifurcations in the third-to-sixth generations of the lung and concluded that the airflow outside the immediate vicinity of the bifurcation was unaffected by the rounding. Therefore, no rounding of the bifurcation was performed in this work.

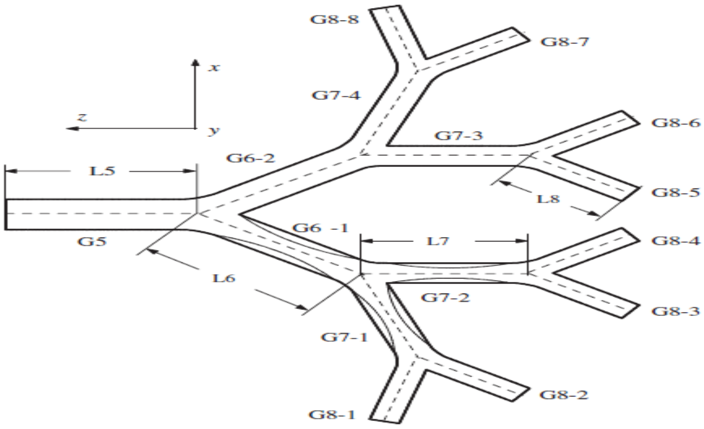

Fig 3.2: The schematic view of the computational model.

Table 3.1: List of Parameters of Geometry

Generation	Diameter (mm)	Length (mm)
5	3.5	10.7
6	2.8	9.0
7	2.3	7.6
8	1.86	6.4

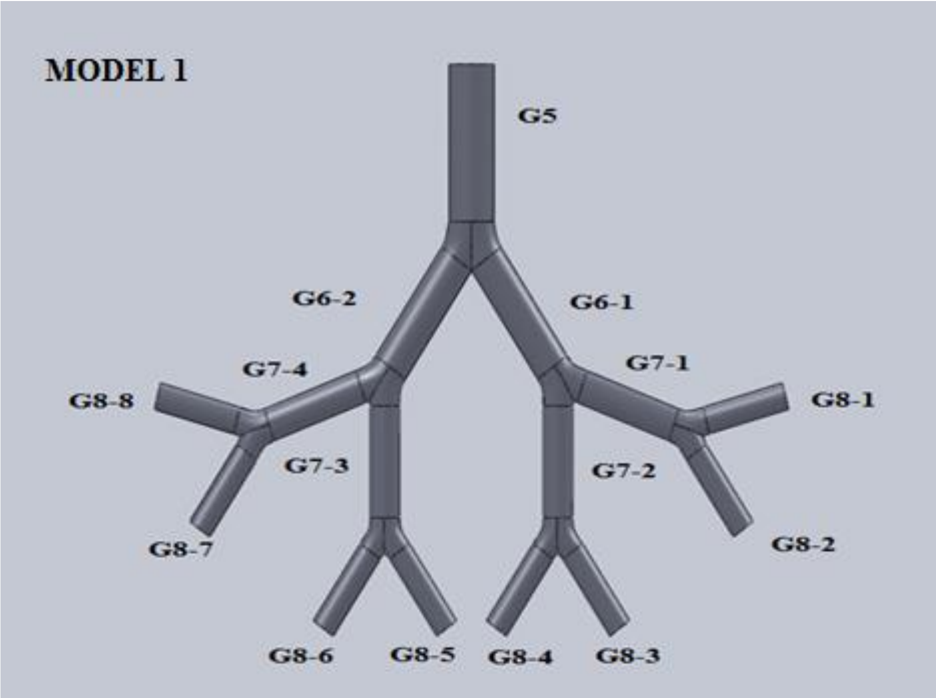
MODEL 1
G5
G6-2
G6-1
G7-4
G7-1
G8-8
G8-1
G7-3
G7-2
G8-7
G8-2
G8-6
G8-5
G8-4
G8-3

a)

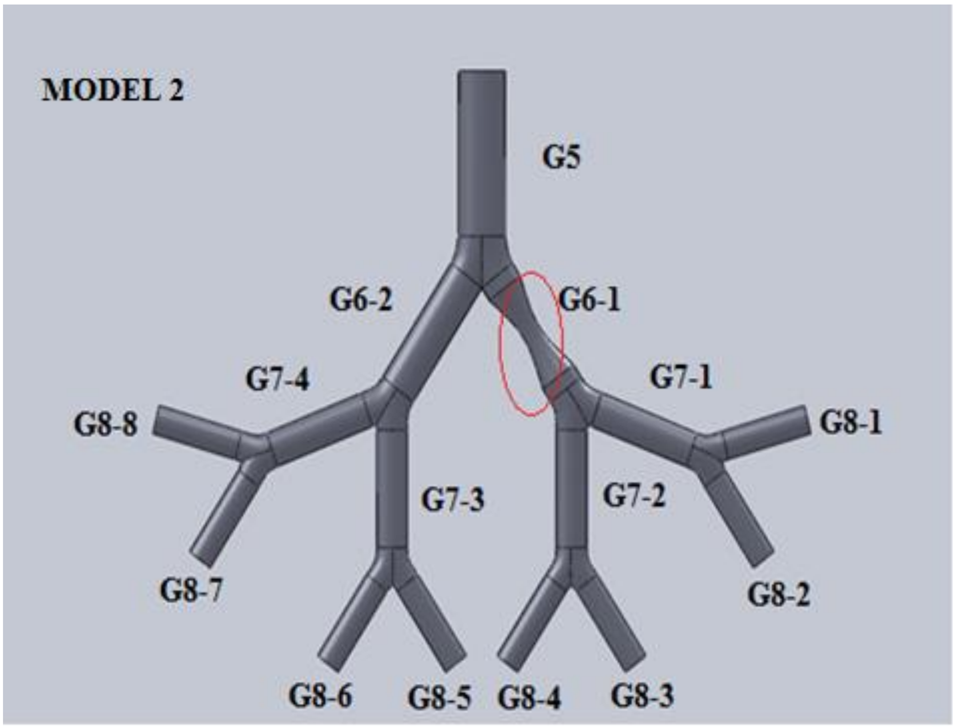
MODEL 2
G5
G6-2
G6-1
G7-4
G7-1
G8-8
G8-1
G7-3
G7-2
G8-7
G8-2
G8-6
G8-5
G8-4
G8-3

b)

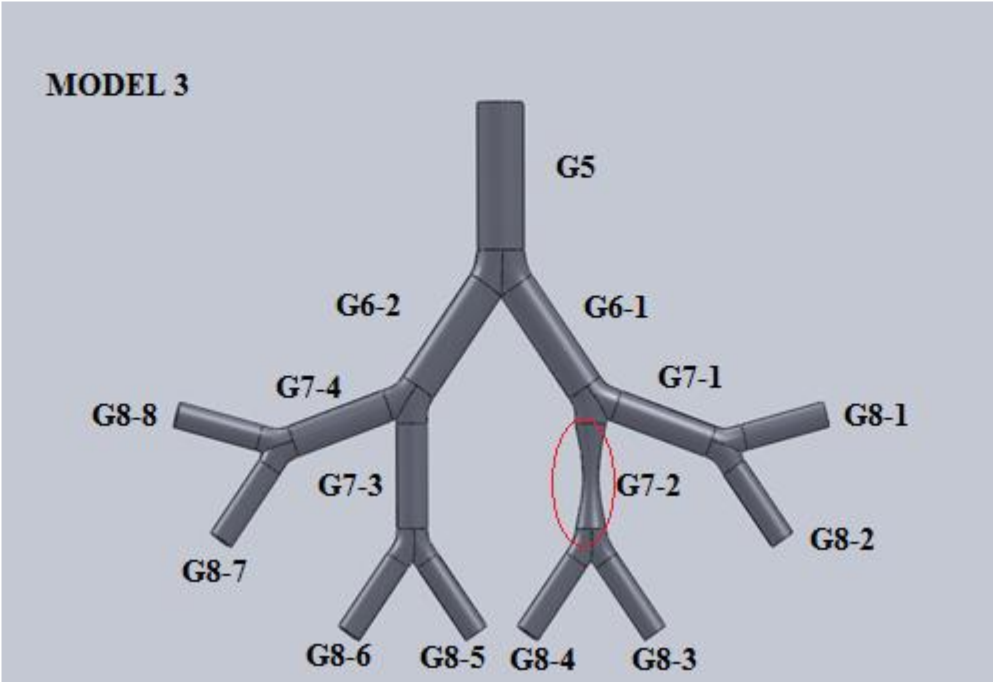

c)

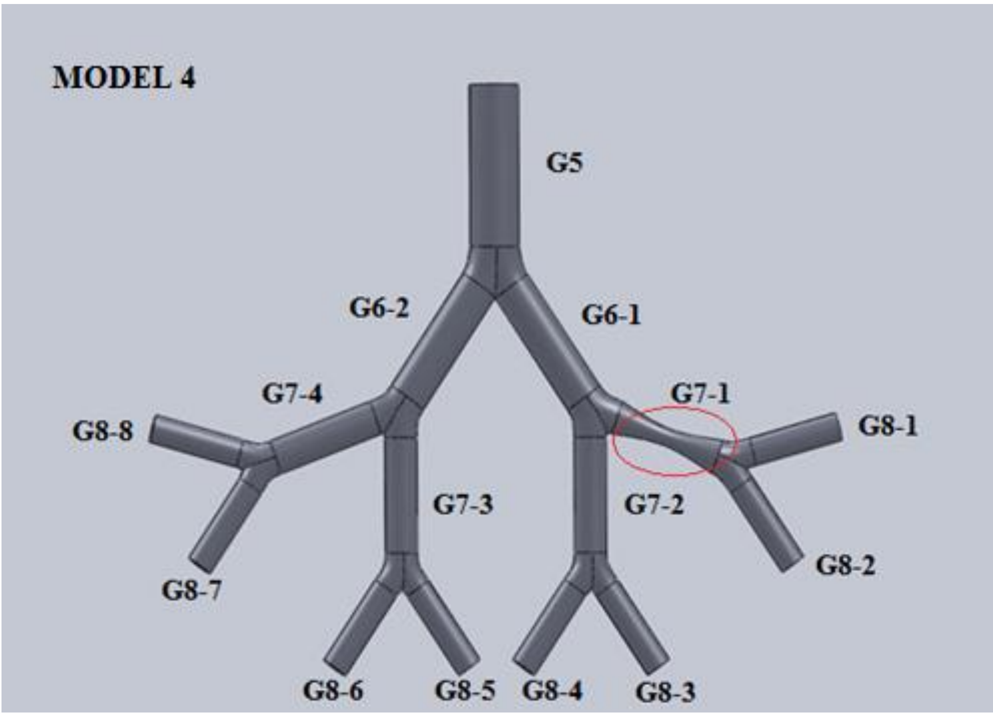

d)

Fig 3.3 : Geometry model of a) healthy model, b) obstructed model at G6-1, c) obstructed model G7-1, d) obstructed model at G7-2)

3.5 MODELLING

The simulations are carried out using eight Reynolds numbers from the range 200 to 1600. This numbers are corresponding to mouth-air breathing rate 0.27- 2.161 l/s. This breathing rate is an average height man breathing condition form quiet to vigorous state. Table 3.2 shows the boundary condition parameters for each condition of breathing. The flow is consider laminar and incompressible. In these equations, $x=(x,y,z)$ is the Cartesian position vector, $u=(u,v,w)$ is the velocity field, and p is the static pressure. All these variables are dimensionless and they are defined with respect to the dimensional variables (denoted here by the superscript *) by $x=x^*/D5$, u=u*/U, and $p=p^*/pU^2$ where U is the mean velocity at the inlet section and D5 is the diameter of the inlet tube. The Reynolds number is define as $Re= \rho UDin/ \mu$, where U is velocity, p is density, u is air dynamic viscosity, Din is inlet diameter.

Table 3.2: Summarized Boundary condition parameters for each condition of breathing

Reynolds Number	**200**	**600**	**1000**	**1400**
Velocity, U(*m/s*)	0.874	2.6218	4.37	6.118
Inlet Diameter(*m*)	0.0035	0.0035	0.0035	0.0035
Outlet Pressure(*Pa*)	101325	101325	101325	101325
Density, $p(kg/m^3)$	1.19	1.19	1.19	1.19
Viscosity,$\mu(kg/ms^{-1})$	$1.82x10^{-5}$	$1.82x10^{-5}$	$1.82x10^{-5}$	$1.82x10^{-5}$

3.5.1 Grid Sensitivity

A grid analysis was done to verify the solver. Three different unstructured mesh and tetrahedral elements (grid 1, grid 2 and grid 3) are being used to analyse the studies from the coarsest mesh to the finest mesh. The grid one cell number is 125000(coarse), grid 2 cell number is 370000(medium) and grid 3 cell number is 520000(fine). The solution for the three grid were shown in figure 2. Graph velocity against local radius of the model. The solutions shows that the different between grid 1 and 2 are 7% and the different between grid 2 and grid 3 are 0.5 %. Hence its proven that cell number more than that 370000 could provide a good results. The cell numbers for the 4 models are 389445, 383439, 388483, and 389855.

a)

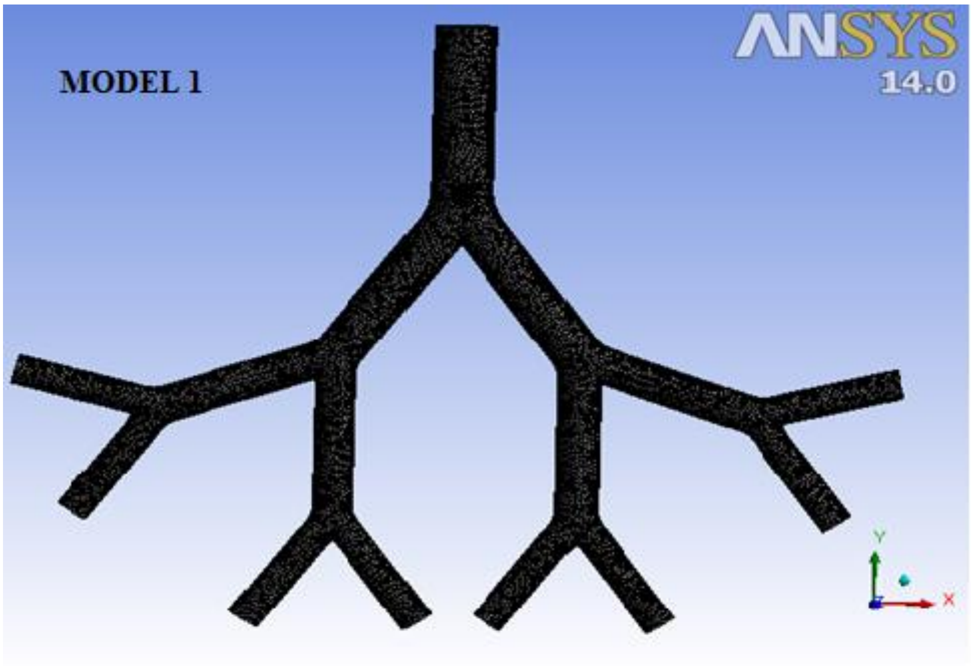

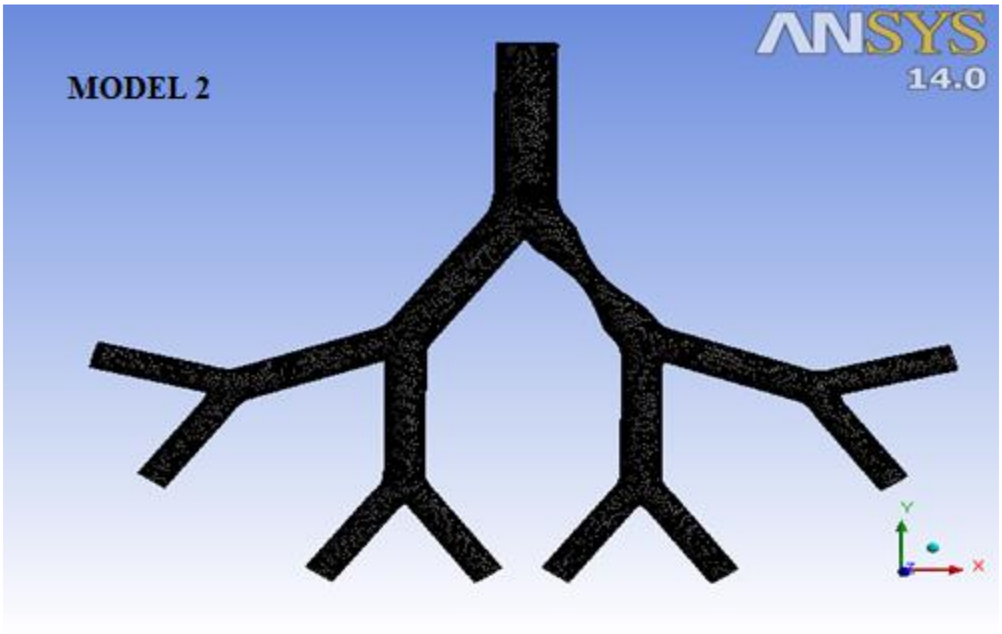

b)

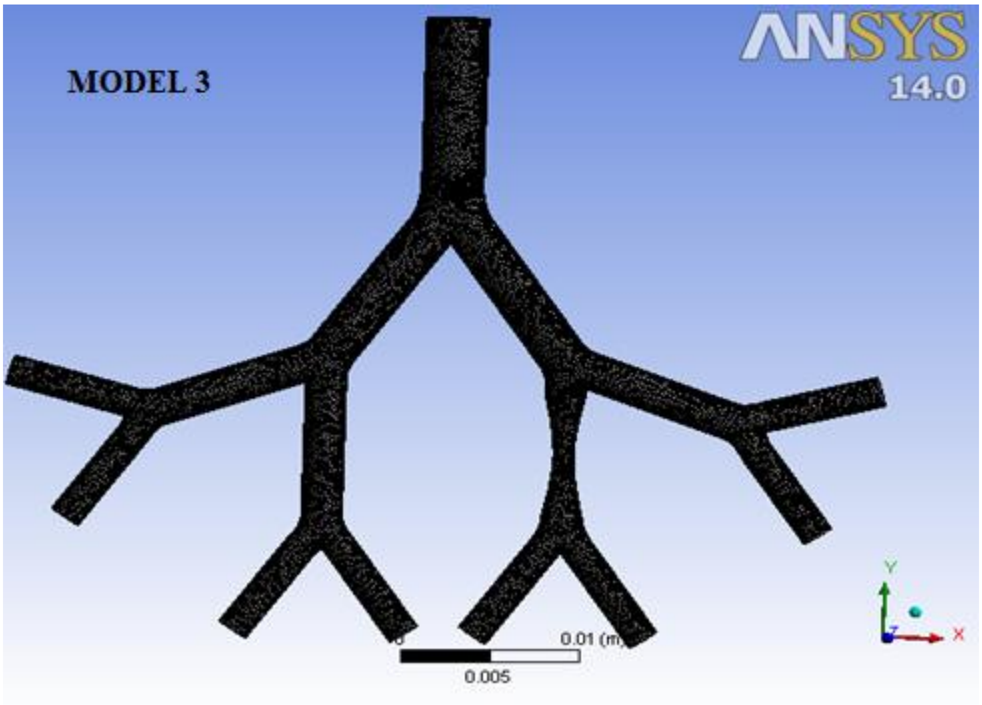

c)

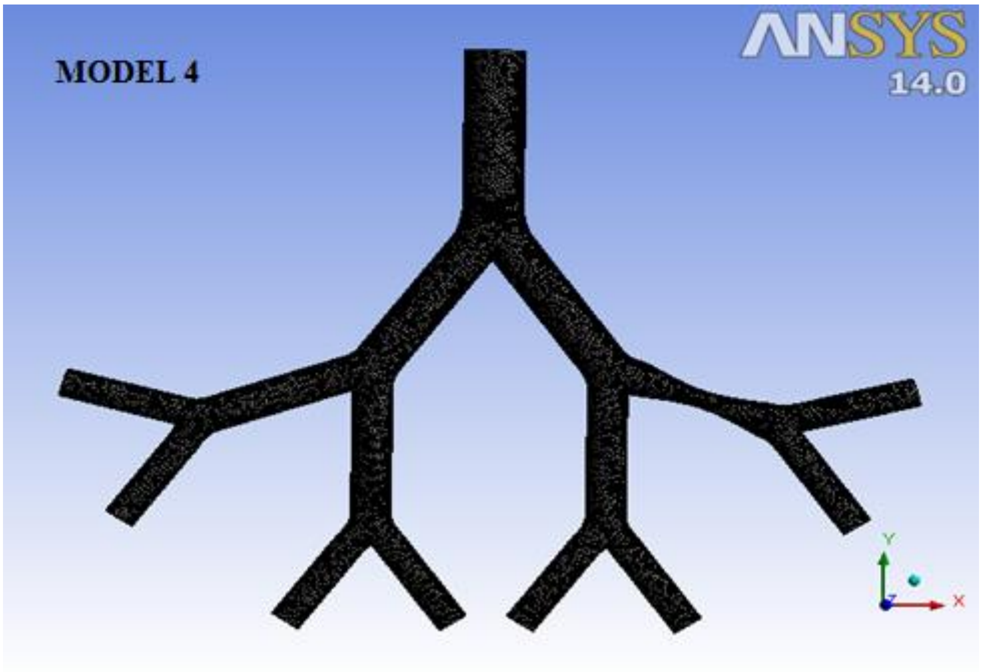

d)

Fig 3.4: Schematic views of the mesh a)model 1, b)model 2, c)model 3 d)model 4

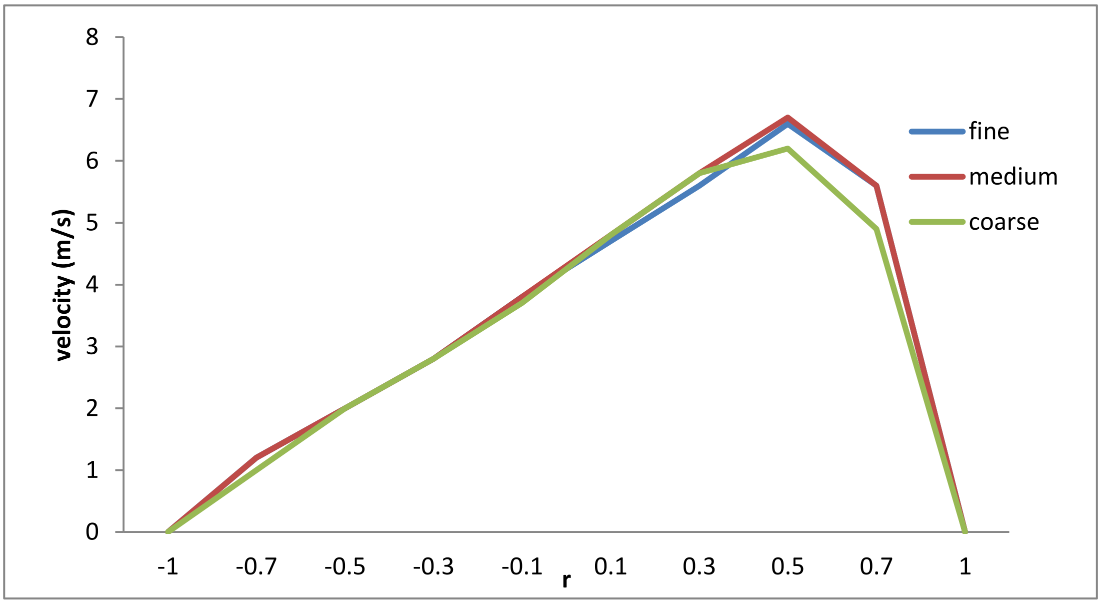

Fig 3.5 : Comparison between different mesh studies of the axial velocity at the end of the second-generation tube in a three-generation airway.

3.5.2 Validation

This numerical model is validated by comparing the present studies with one experimental data and numerical data. In the experiment (Zhao and lieber) data, the steady laminar flow pass through a two generation bifurcation plane. The diameter of the mother branch is 3.51 cm and the total cross-sectional area of the two daughter branches is the same as that of the mother branch. The junction radius of curvature is 7 times the diameter of the daughter branch. The bifurcation angle is 70 degree. The velocity measurement had been carried out in the vertical plane and bifurcation plane. Reynolds number 500 is specified and the mean velocity calculated using the Reynolds number. The calculated axial velocity is at the end of the second generation bifurcation is compared with the measurement of experimental data (Zhao and Lieber,1994) and numerical result(Y.liu et al., 2002). It can be seen that the agreement between the present results, experimental data and numerical results is excellent, as the velocity is skewed to the inner wall in the bifurcation plane and the M shaped velocity distribution in the Transverse plane. Therefore, the numerical scheme is capable of reproducing the bifurcation flow behaviour in the symmetrical airway.

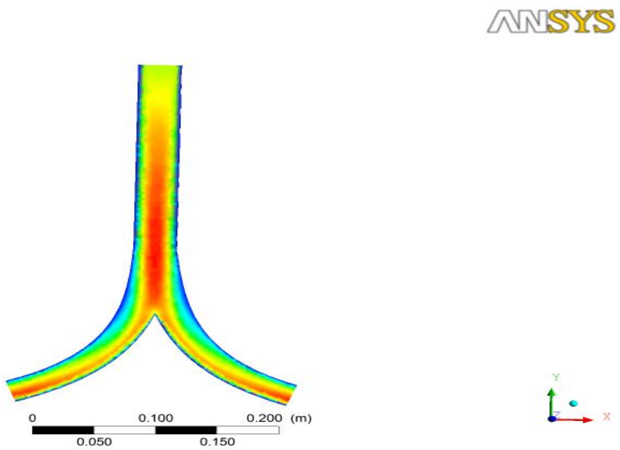

Fig 3.6: Geometry of the symmetric bifurcation model, based on Zhao and Lieber (1994) study. The axial velocity distribution at Reynolds number 500.

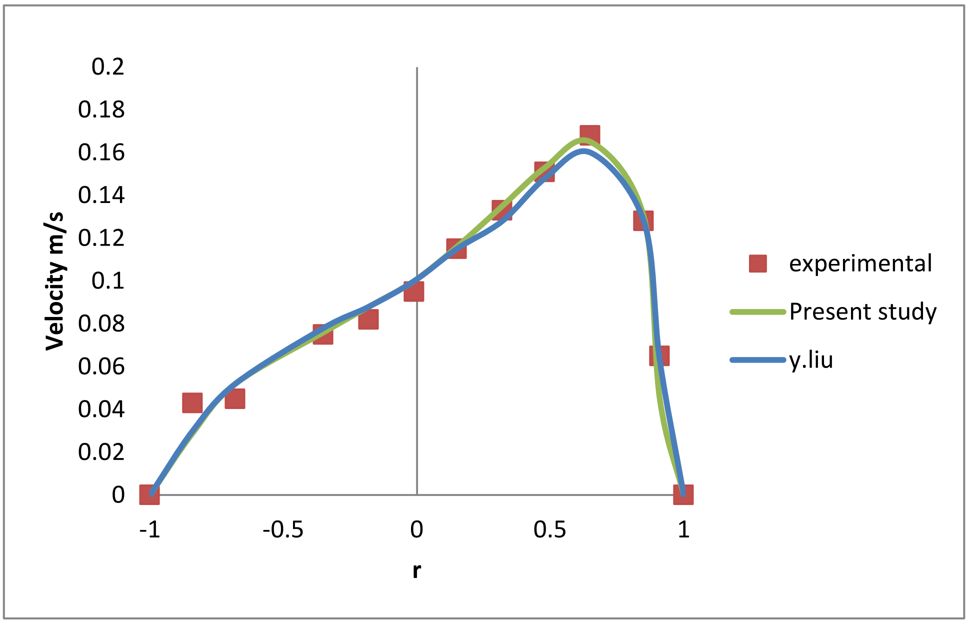

a)

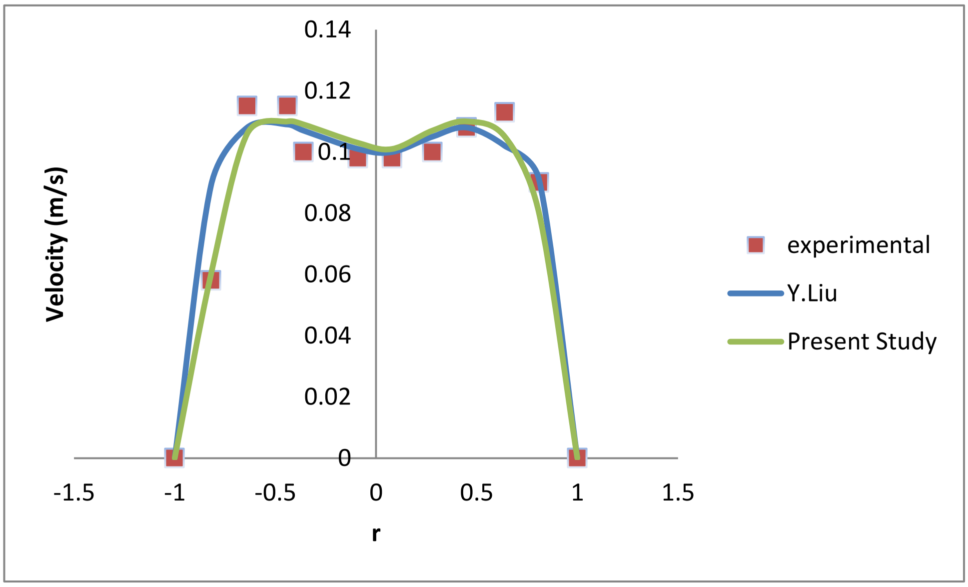

b)

Fig 3.7: Comparison between calculations and measurements (Zhao and Lieber, 1994) ,(Y.liu et al., 2002) and present studies of the axial velocity at the end of the second-generation tube in a three-generation airway with Re =500: (a) bifurcation plane and (b) vertical plane.

CHAPTER 4

RESULTS AND DISCUSSION

4.1 INTRODUCTION

In this chapter, obtained results were analysed and discussed. The effect of COPD, mass flow rate ratio and pressure dropped are being discussed here. After validating the numerical results, the next step is to investigate the effect of COPD on the airflow. Four Reynolds numbers (200, 600, 1000,1400) are choose to run the simulation. The Reynolds number is define as $Re = \rho V D_{in} / \mu$, ρ which is density, *Din* is inlet diameter, μ is dynamic viscosity and V is velocity.

4.2 FLOW PATTERN

The effect of COPD is investigated by studying the normal and obstructed model. The normal model (model 1) is studied by showing the streamline velocity of two Reynolds number Re 200 and 1600. As the airflow from 1st generation goes to 2nd generation, the centrifugal force pushes more air towards the inner wall. In 7th generation airway, more air enters the medial branch than lateral branches as the air skewed to the inner wall. The lateral branches are much weaker than the medial branch. Hence, more air also will enter into medial 8th generation branch than the lateral which much weaker. As the increased in Reynolds number the skewed to inner wall is much more significant in the lower branches. The axial velocity in lower Reynolds number (Re=200) couldn't produce M shape graph. As increased in Reynolds number the M shaped are more visible indicating stronger flow.

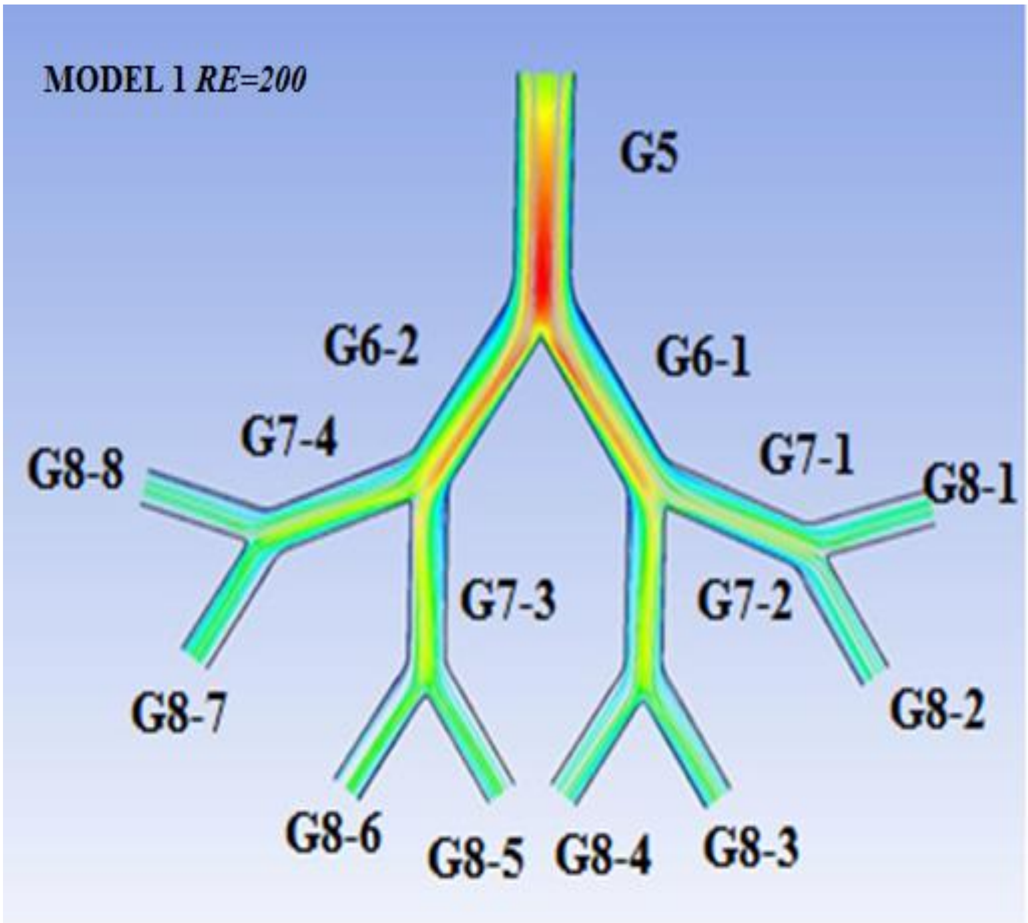

a)

b)

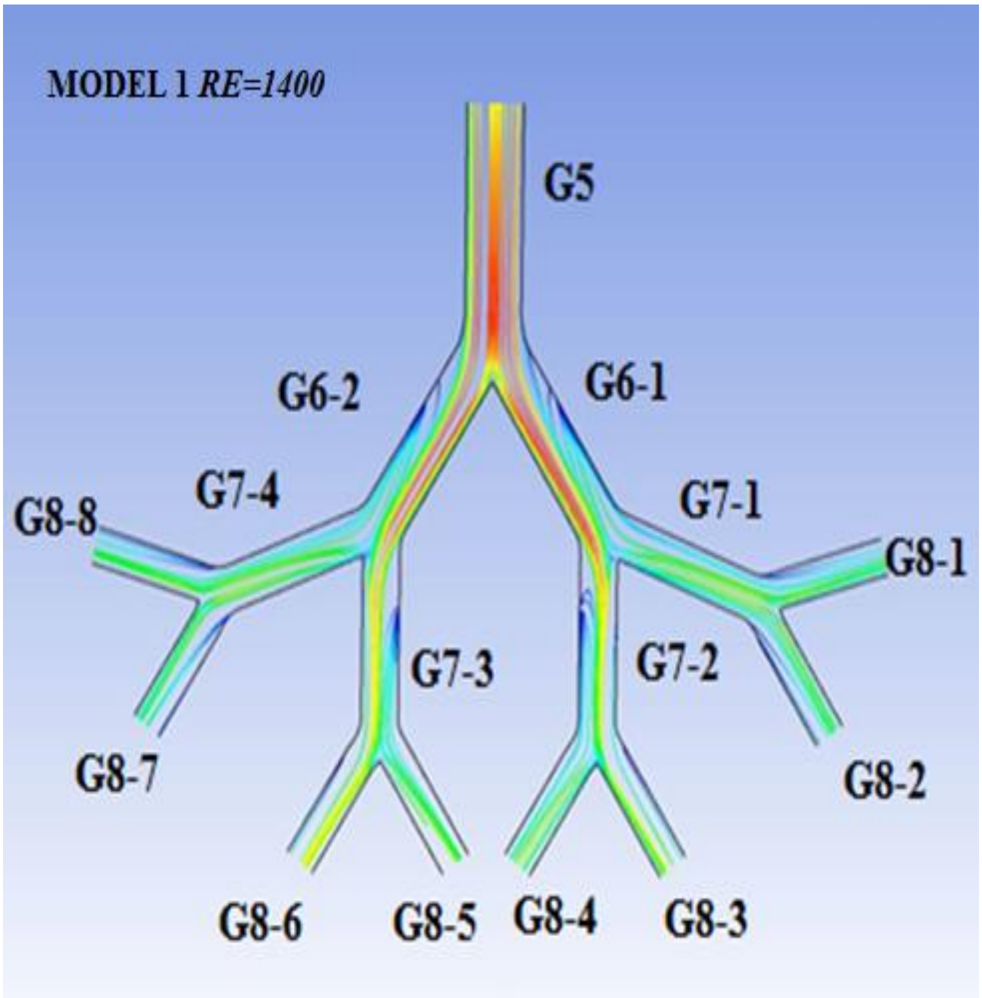

Fig.4.1: The flow patterns of model 1: (a) flow vectors of Re =200; (b) flow patterns of Re = 14000

When one of the airflow in G6 is obstructed, it will indirectly alter the airflow pattern. In model 2, as the airflow enters G5 and split at the bifurcation, less air will enters the G6-1 than G6-2 because of the obstructed region in the G6-1. The maximum velocity is skewed to the inner wall because of centrifugal force. As the air move across the G6, it will split at bifurcation and enter the daughter branches. The velocity accelerates through the throat which in converging diverging nozzle shaped. The stream flow forms jet flow and the lowest pressure is in the middle of the part G6-1. The velocity in the middle of the G6-1 is the highest which is the obstructed airway and exceeds the velocity in the G5.The obstructed airway behaves like a jet, as this jet effect are increased in momentum and the skewed velocity profile length are short to recover back before the 2nd bifurcation. Hence most of the air will enter medial branch g7-2 and the flow in the lateral branch is very weak. As increased in Reynolds number the jet effect become much stronger. In higher Reynolds numbers the air circulation and stagnation zone are form in G6-1 are much more visible while no flow separations in G6-2. The recirculation will block the air to enter the lateral branch. In the obstructed branch G6-1, most of the air wil enter the medial branch G7-2 as the flow skewed to the inner wall and less amount of air will enter the lateral branch G7-1. Hence this explain a deep breath doesn’t help a COPD patient. A COPD patient should breathe in gently and slowly as it can reach every alveolus in the lungs.

a)

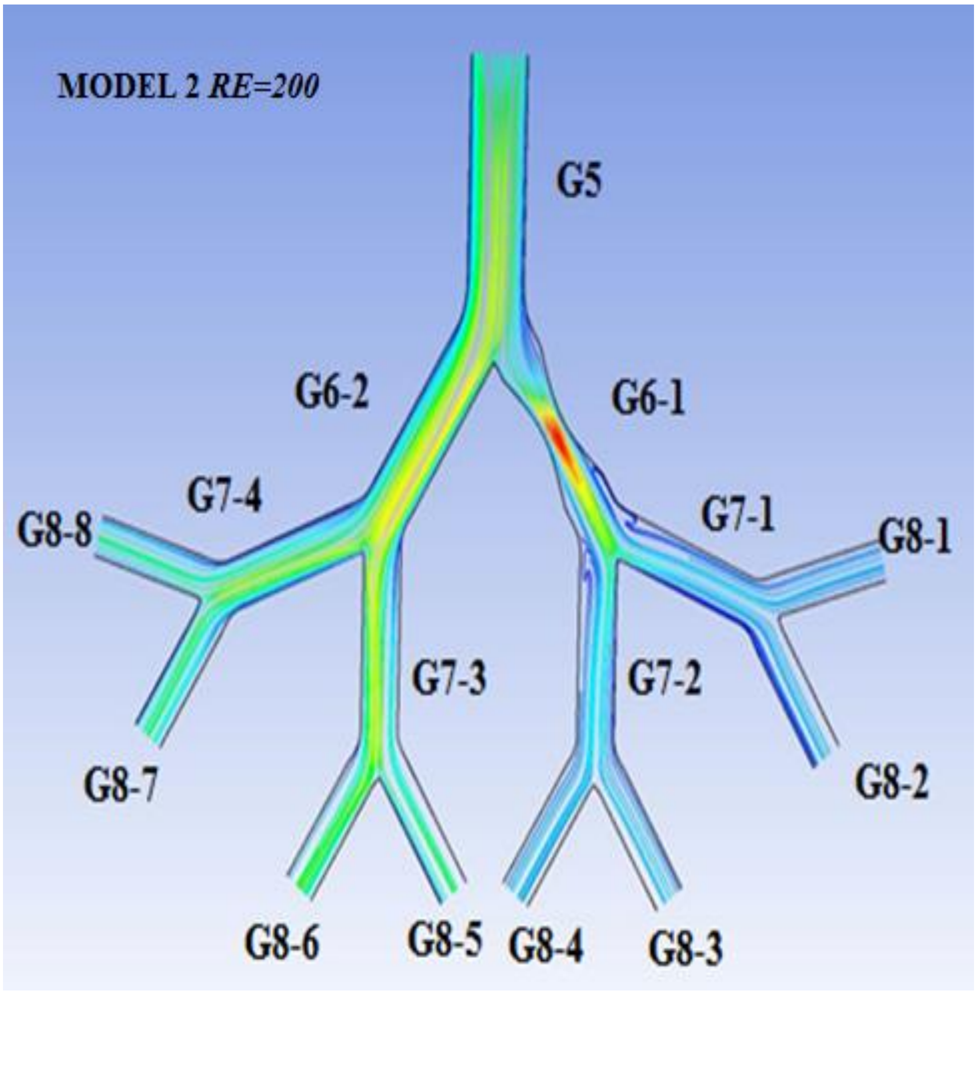

b)

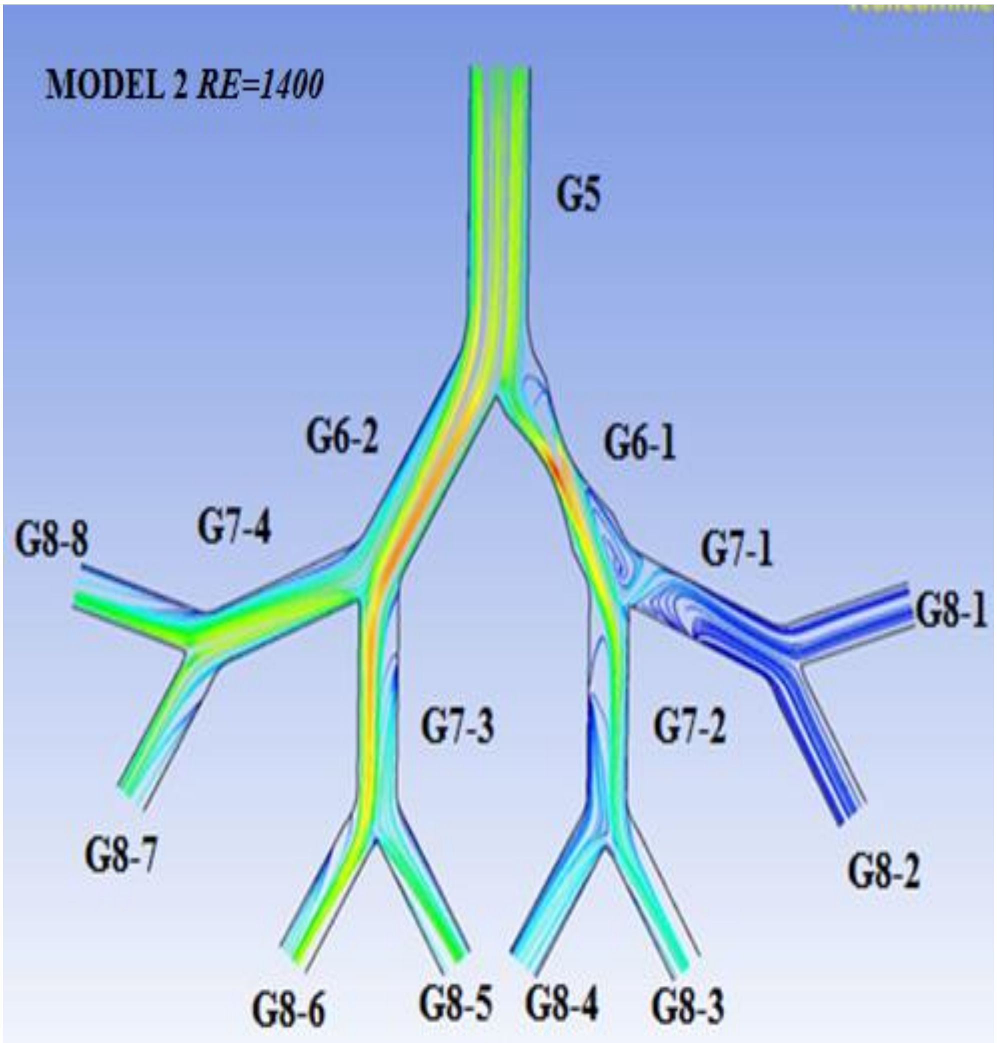

Fig. 4.2: The flow patterns of model 2: (a) flow vectors of Re =200; (b) flow patterns of Re = 14000

In figure 5, the flow pattern of airway model 3 is shown in which the branch in G7-2 is consider obstructed. Most of the air will enter the lateral branch because of the obstruction in G7-2, even the flow is skewed to the inner wall as the length of G7-2 is not enough to recover due to high momentum. The obstructed airflow behaves like a jet which could produce a symmetrical velocity profile at the outlets G8-3 and G8-4. As increased in Reynolds number, the momentum in jet flow also will increase and the velocity profile will skew more to inner wall. From the figure, it can be seen that the obstruction at G7-2 could produce recirculation in both downstream and upstream airways.

a) 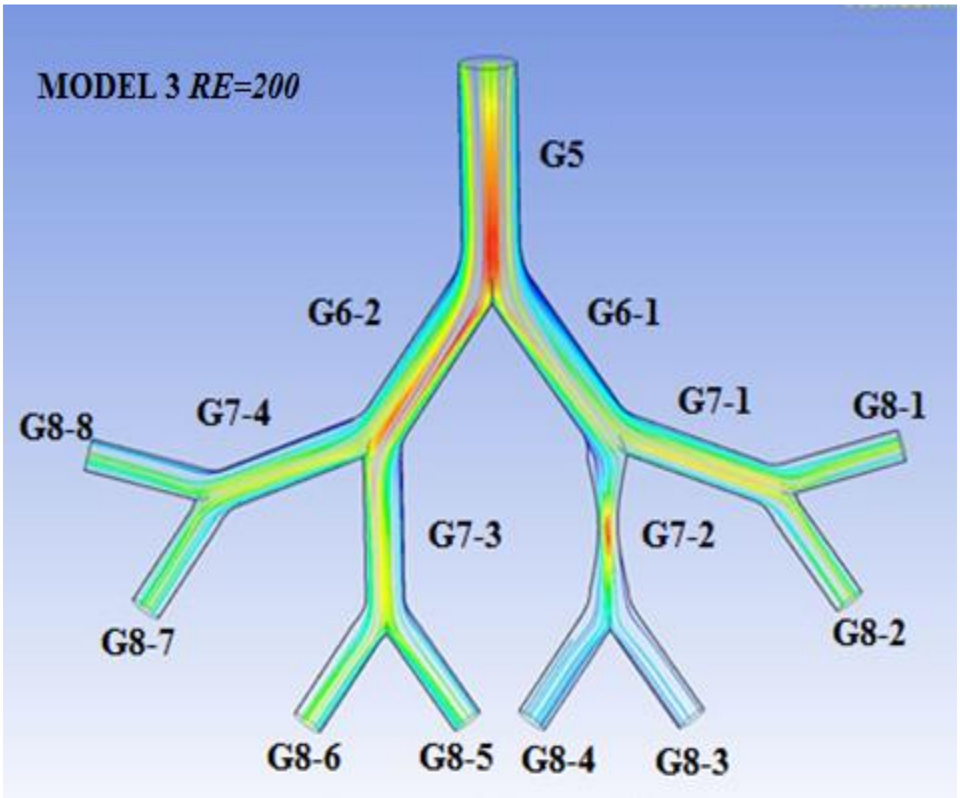

b) 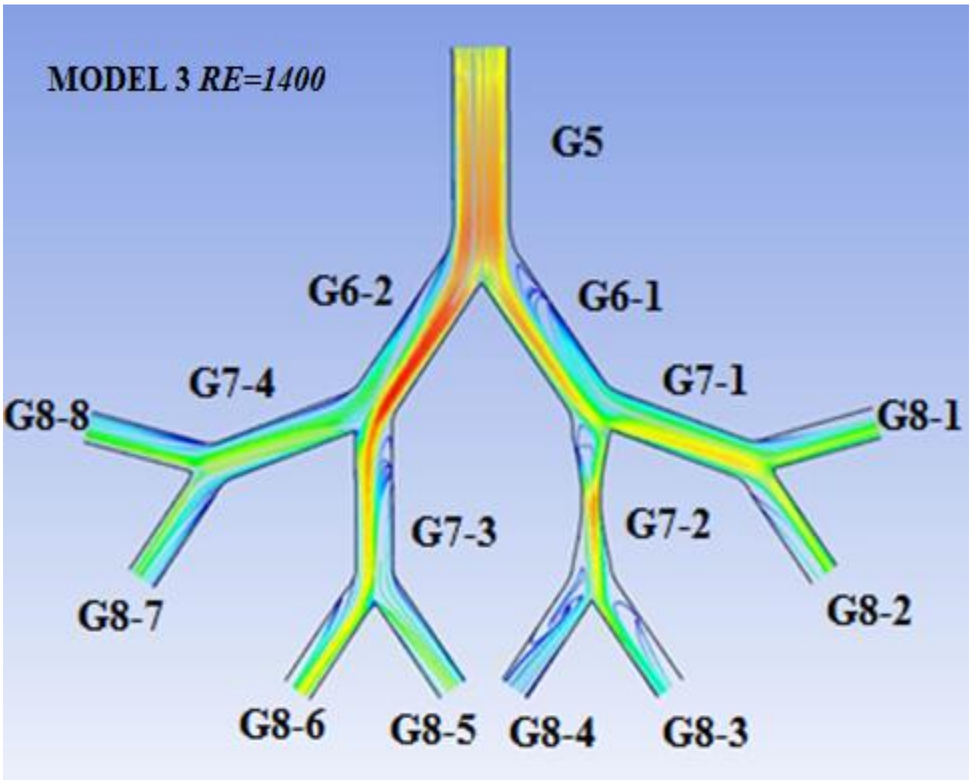

Fig. 4.3: The flow patterns of model 3: (a) flow vectors of Re =200; (b) flow patterns of Re = 1400

The results below shows the behaviour of airflow of model 4 which is the the lateral airway is obstructed G7-1. In this case most of the air enters the medial branch G7-2, because of obstructed airway in G7-1 and the centrifugal force in G6-1. As the Reynolds number increase, more air is skewed to the medial branch which are from G6-1 to G7-2. Since the air flow in the airway is weak the in G7-1, the obstructed airways makes the velocity profile at the end of G7-1 almost symmetrical. Although the air flow is weak in the lateral branch, recirculation still happens at the entrance of G8-1 and G8-2. The recirculation also considered as weak recirculation. Hence it indicates that the obstruction in G7-1 not only produce a symmetrical airway in daughter branch but also a stagnation region in G6-1. The obstruction in G7-1 could affect both down and upstream airways.

a)

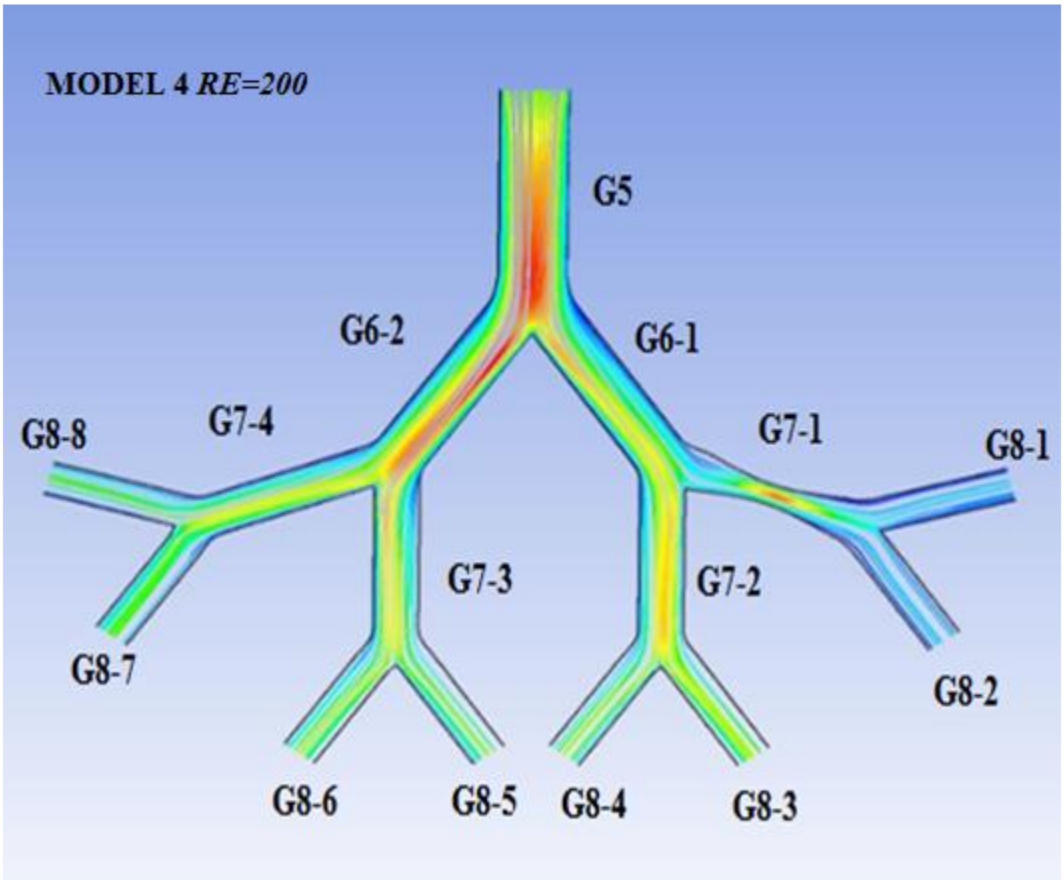

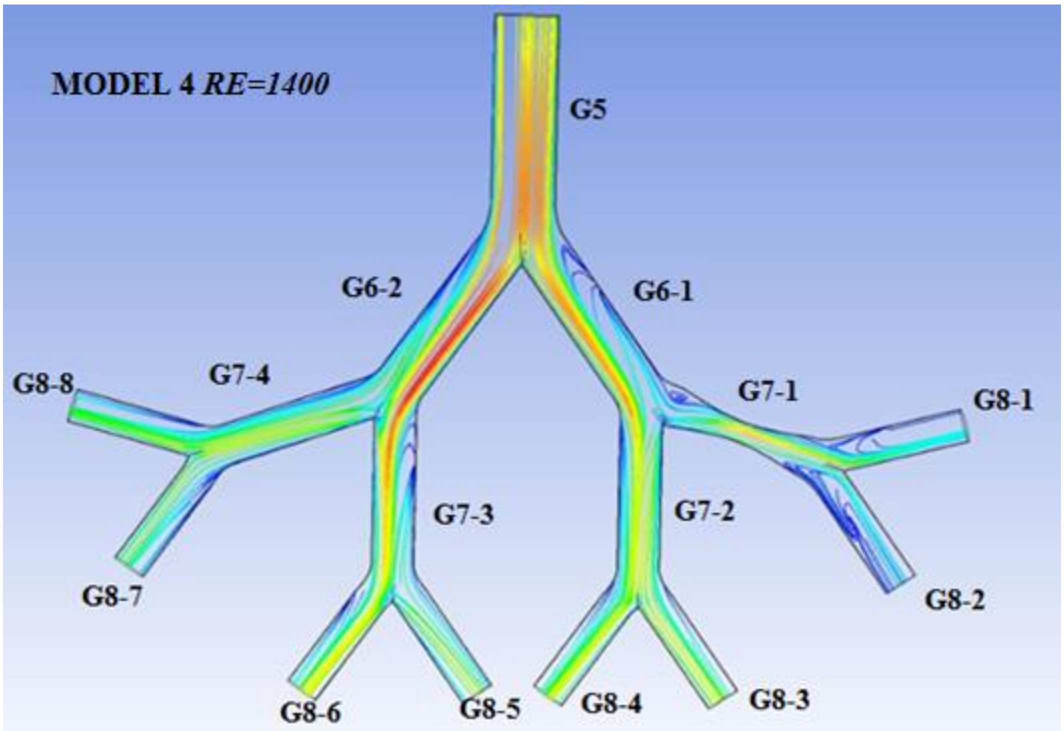

b)

Fig. 4.4: The flow patterns of model 4: (a) flow pattern of Re =200; (b) flow patterns of Re = 1400

4.3 MASS FLOW PARTITION

In a four generation healthy airway model, a parabolic velocity at the inlet leads to equal fluid flows in the fourth generation branches. Nevertheless, the velocity profile skewed to the inner wall in the lower generation airway and more fluid will enter the medial branches than the lateral branches. This behaviour will contribute to imbalance flow partition throughout the medial and lateral branches. Hence, the obstruct presence in the airway could make the imbalance much worst. The imbalance in flow partitioning is measured by *m* which is defined as the ratio of the mass flow rate

$$\dot{M}i, j = \frac{\dot{m}i}{\dot{m}j}$$

Table 4.1: Ratio of mass flow rate *ṁ6-1/ṁ5*

	Flow rate ratio *ṁ6-1/ṁ5*			
Reynolds No.	**Model 1**	**Model 2**	**Model 3**	**Model 4**
200	0.47	0.25	0.407	0.406
600	0.48	0.236	0.404	0.409
1000	0.478	0.236	0.405	0.406
1400	0.479	0.236	0.402	0.404

Table 4.2: Ratio of mass flow rate *ṁ7-1/ṁ6-1*

	Flow rate Ratio *ṁ7-1/ṁ6-1*			
Reynolds No.	**Model 1**	**Model 2**	**Model 3**	**Model 4**
200	0.472	0.478	0.75	0.23
600	0.44	0.34	0.75	0.22
1000	0.435	0.198	0.72	0.215
1400	0.425	0.08	0.72	0.213

In figure 4.5, shows the mass flow rate ratio from branch G6-1 to branch G5 against Reynolds number. In the graph, it can be seen that the influence of the obstruction on flow partition in the obstructed airway. In model 1, the G6-1 branch takes 48% of the total flow rate which is almost half of the total flow rate as the two branches separated G6-1 and G6-2. It indicates that the flow rate is balanced and symmetric. However in model 2, the G6-1 branch takes about 25% of the total flow rates and it happen because of the obstruction in G6-1. Hence most of the fluid will enter G6-2 and indicates an imbalances flow rate. In model 3 and 4, the ratio of the flow rate is lesser than model 1 which are around 40% because of obstruction in third generation G7-1 and G7-2. The flow rate ratio in model 3 and 4 are almost identical.

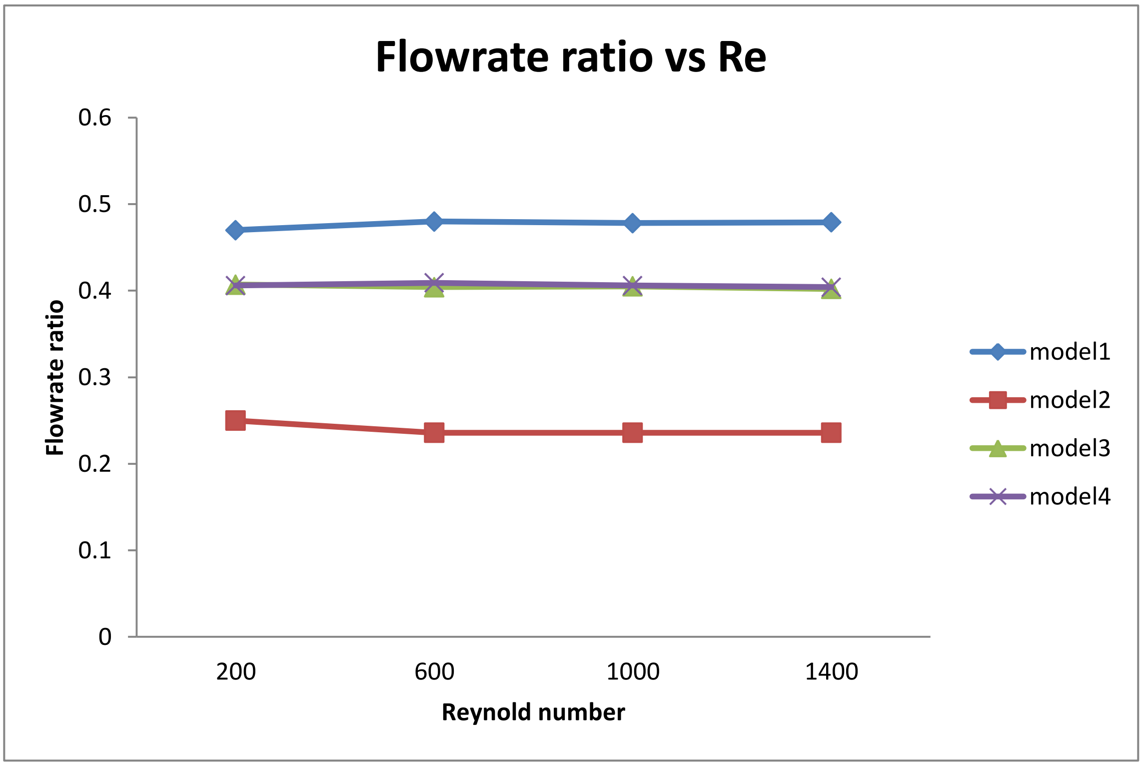

Fig 4.5: The variation of mass flow ratio of ṁ6-1/ṁ5 with Re.

In figure 4.6, it shows the mass flow rate ratio from branch G7-1 to G6-1 against the Reynolds number. Reynolds number might affect the airflow partition. In model 1, the flow rate is lesser in G7-1 the lateral branch than the medial branch G7-2 because of centrifugal effect which makes the flow of the air skewed to the inner wall. In another case which is the model 2, the air flow ratio decreases when the Reynolds number increase. In this case, it can be explained that the obstruction G6-1 cause recirculation at the end of G6-1 branch, which will blocks the air from entering G7-1. As the Reynolds number increase, the high momentum fluid enhanced stronger recirculation at the end of G6-1 branch. In model 3, the air flow ratio is about 75% because of obstruction in medial branch G7-2, which blocks the air to enter the medial branch and more air enters the lateral branch G7-1. While in model 4, the air flow ratio is about 23 % as the lateral branch G7-1 is obstructed and less air enters into it.

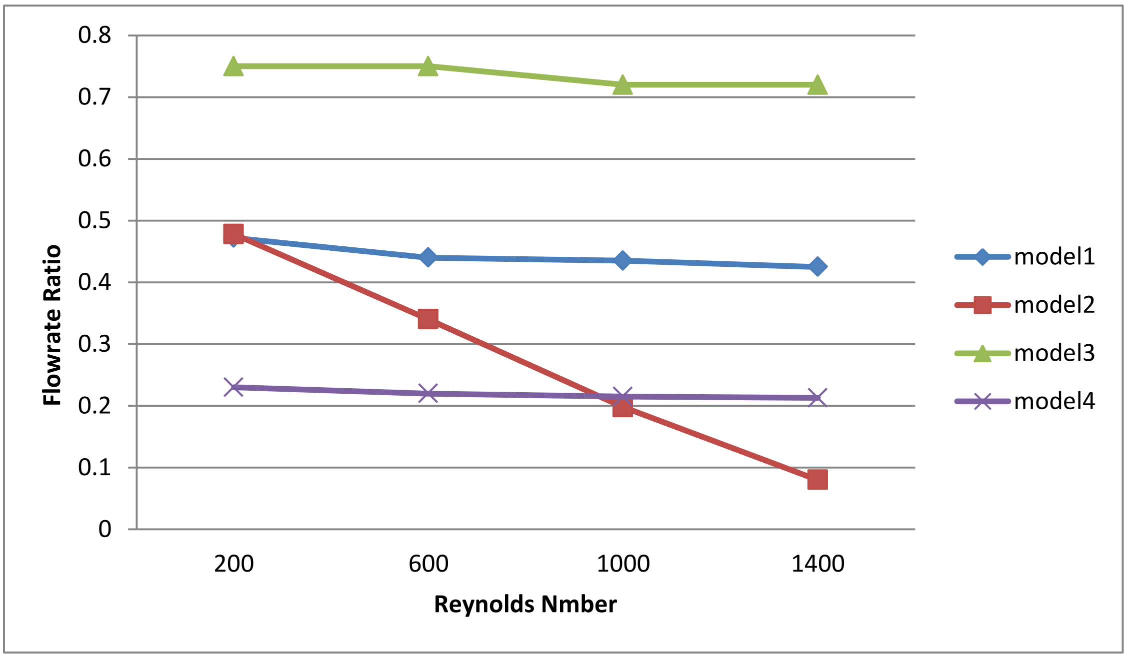

Fig 4.6 : The variation of mass flow ratio of ṁ7-1/6-1 with Re

4.5 PRESSURE DROP

The change of pressure in airways plays an important role in human respiratory process. The respiratory process can only take place continually and normally when the alternative contraction and expansion of the respiratory muscles overcomes the pressure drop due to viscous and other losses. In this present study, the pressure drop is define as

$$\Delta P = \frac{Pin}{Pout}$$

In this study *Pin* is the mass weighted integral of total pressure over inlet and *Pout* is the mass weighted integral of total pressure over the eight outlet sections in the fourth generation branches. A graph of Pressure drop versus Reynolds number had been plotted in the figure below. The pressure drop normally will increase with increasing in Reynolds number, as it is consistent with Bernoulli's equation. In the graph, it can be seen that the pressure drop in model 2 increase much higher than the models. Model 3 and 4 have almost similar pressure drop because the obstruction happen at third generation and Model 1 have the lowest pressure drop. The most likely explanation of this phenomenon is that the diameter reduction of model 2 is the biggest and this results in a much higher flow resistance, particularly for the low momentum fluid. This also explains why the COPD patients feel difficult to take breath.

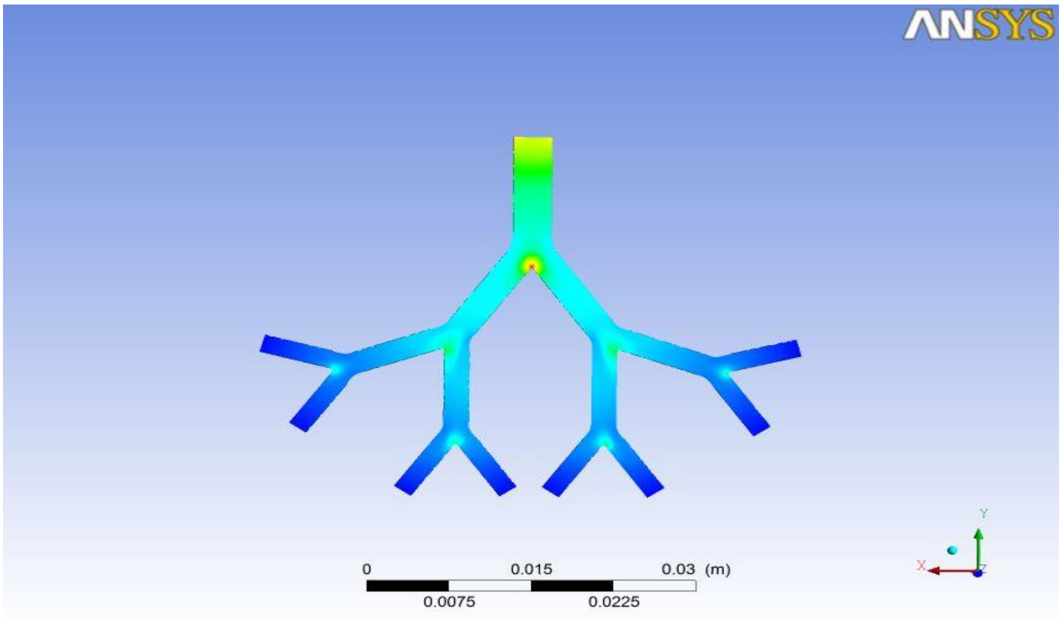

Fig 4.7 : Pressure Distribution in Model 1 (Re:1000)

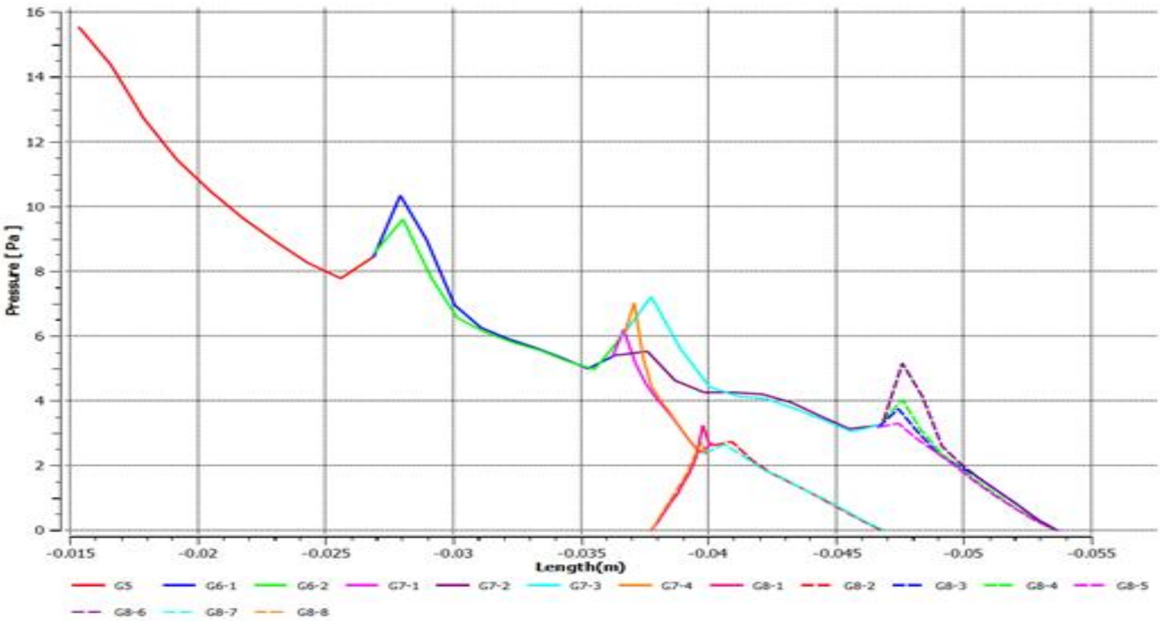

Figure 4.8: Pressure Distribution graph in model 1 (Re:1000)

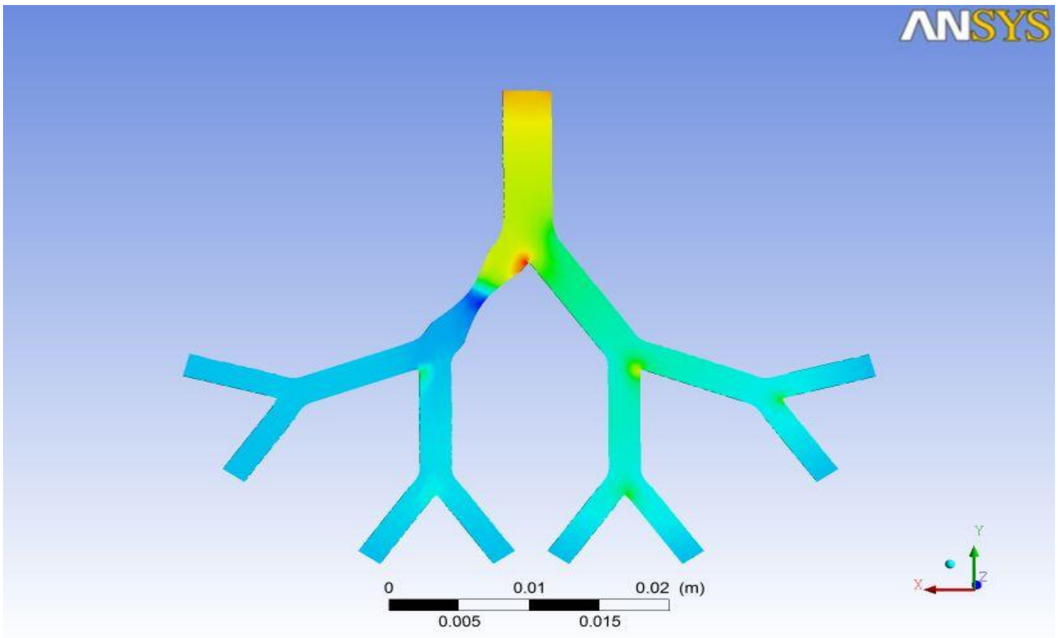

Figure 4.9 : Pressure distribution in model 2 (Re= 1000)

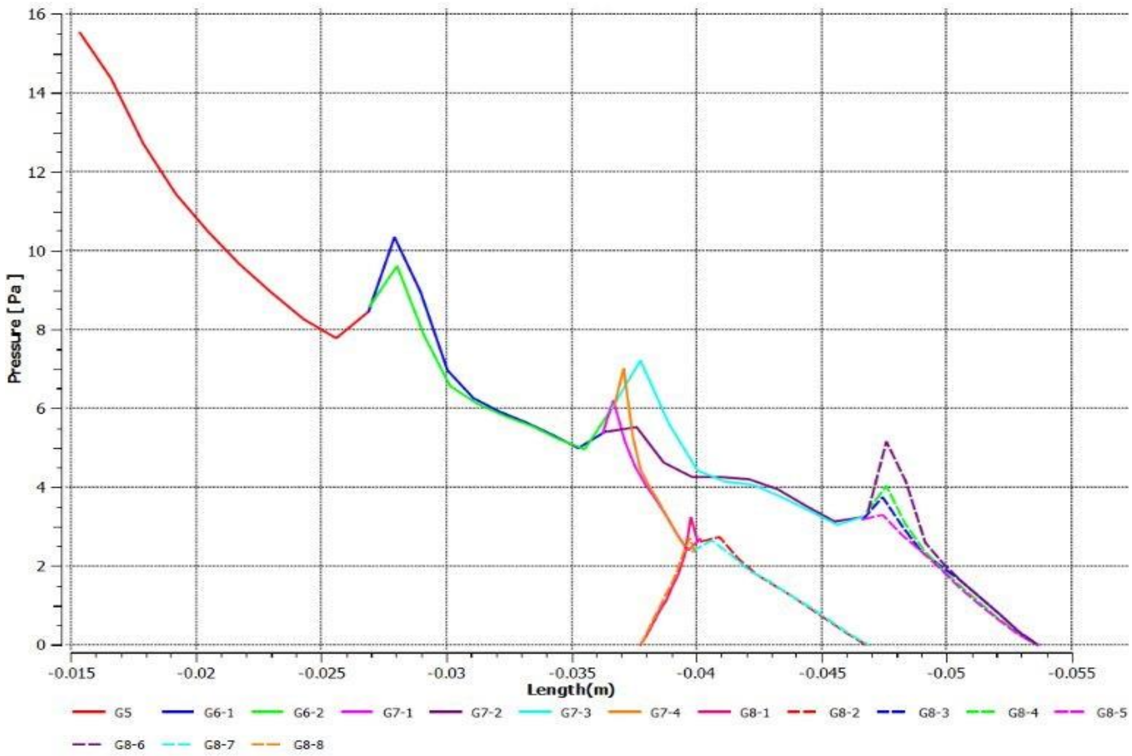

Figure 4.10: Pressure distribution graph from G5 to G8 in model 2 (Re=1000)

Table 4.3: Pressure Drop Table

Reynolds Number	Model1(Pa)	Model2(Pa)	Model3(Pa)	Model4(Pa)
200	2.7433	3.833	3.051	3.04
600	11.52	17.147	13.0226	12.86
1000	24.022	36.4068	27.32	26.88
1400	39.77	60.3122	45.18355	44.405

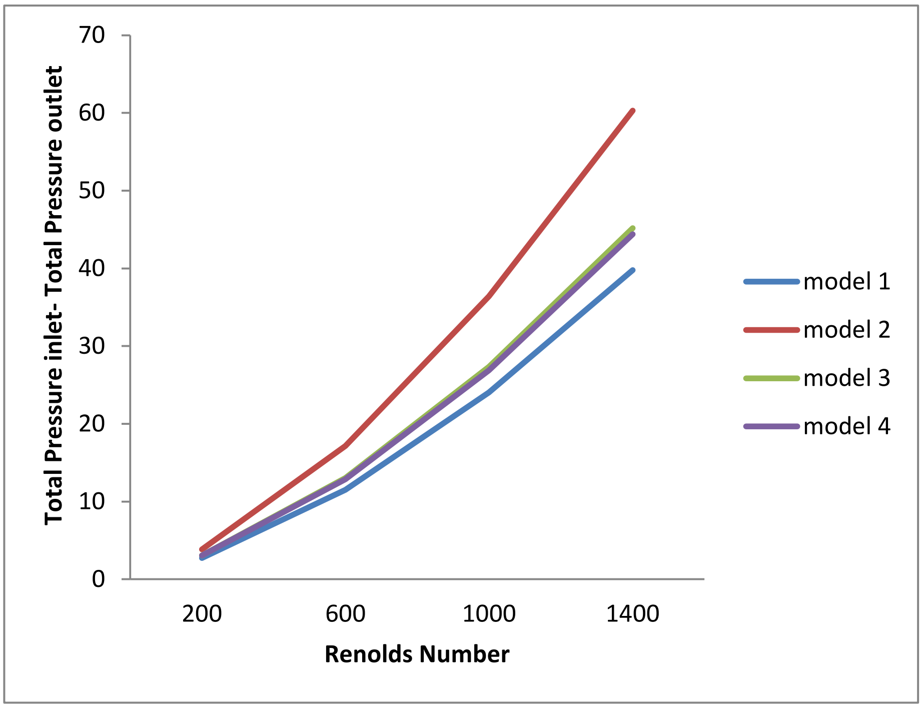

Fig 4.11: The variation of pressure drop with Re.

CHAPTER 5

CONCLUSION

5.1 CONCLUSION

The effect of COPD on respiratory flow is numerically studied on four different four-generation models. The fully three-dimensional incompressible laminar Navier–Stokes equations are solved by a CFD solver. The numerical calculation leads to the following conclusions:

The obstructed airway alters the flow field significantly, a strong separation region exists behind the ‘‘throat’’ at higher Reynolds number. In a bifurcation airway, the obstruction may generate recirculation both upstream and downstream. These re-circulation cells block the air from entering the downstream branches which indicates that a deep breath may block the oxygen from reaching the alveoli for a COPD patient.The obstructed airway has significant influence on the daughter branches and it increases the flow resistance significantly.

5.2 RECOMMENDATION

Since Computational Fluid Dynamics is one of the best tools to study on related issues of human airways, it would be beneficial to concentrate on the following issues in the future research:

i. Study on particle and aerosol deposition in human airways.

ii. Modelling off plane airway of human airways.

iii. Comparison study on simplified and real human airway models.

REFERENCES

[1] Arpad Farkas, Imre Balashazy (2006). Simulation of the effect of local obstructions and blockage on airflow and aerosol deposition in central human airways.

[2] Clement Kleinstreuera,, Zhe Zhanga, Chong S. Kimc.(2003) Combined inertial and gravitational deposition of microparticles in small model airways of a human respiratory system

[3] Clement Kleinstreuera, Zhe Zhanga, Zheng Li.(2005) Modeling airflow and particle transport/deposition in pulmonary airways.

[4] Honglin Zhang, GeorgePapadakis (2010). Computational analysis of flow structure and particle deposition in a single asthmatic human airway bifurcation.

[5] H.Y. Luo, Y. Liu, X.L. Yang.(2007) Particle deposition in obstructed airways.

[6] J.W. De Backer, W.G. Vos, C.D. Gorl, P. Germonpr´,B. Partoens , F.L.Wuyts , P.M. Parizelc, W. De Backer.(2001) Flow analyses in the lower airways: Patient-specific model and boundary conditions.

[7] Kiao Inthavonga, Lok-Tin Choia, Jiyuan Tua,, Songlin Dinga, Francis Thien.(2007) Micron particle deposition in a tracheobronchial airway model under different breathing conditions.

[8] Marie Bruyneel , Valérie Jacob, Christina Sanida, Lieveke Ameye, Roger Sergysels , Vincent Ninane .(2002) Hoover's sign is a predictor of airflow obstruction severity and is not related to hyperinflation in chronic obstructive pulmonary disease

[9] Maria Chiara Piglione, Daniela Fontana, Marco Vanni. (2012). Simulation of particle deposition in human central airways.

[10] Martin A. Nagels, John E. Cater. (2009). Large eddy simulation of high frequency oscillating flow in an asymmetric branching airway model.

[11] Min-Yeong Kang, JeongeunHwang, Jin-WonLee (2011). Effect of geometric variations on pressure loss for a model bifurcation of the human lung airway.

[12] Mihai Mihaescu a,n, GouthamMylavarapu, EphraimJ.Gutmark, NelsonB.Powell (2011) Large Eddy Simulation of the pharyngeal airflow associated with Obstructive Sleep Apnea Syndrome at pre and post-surgical treatment.

[13] P. Worth Longest, Samir Vinchurkar (2007). Effects of mesh style and grid convergence on particle deposition in bifurcating airway models with comparisons to experimental data.

[14] Rainhill K. Freitas, Wolfgang Schroder (2008). Numerical investigation of the three-dimensional flow in a human lung model.

[15] X.L.Yanga,Y. Liua,, R.M.C. Soa, J.M.Yangb.(2003) The effect of inlet velocity profile on the bifurcation COPD airway flow

[16] Xiaole Chen, Wenqi Zhong, Baobin Sun, Baosheng Jin , Xianguang Zhou.(2011) Study on gas/solid flow in an obstructed pulmonary airway with transient flow based on CFD–DPM approach.

[17]Xiaole Chen, Wenqi Zhong, Xianguang Zhou, Baosheng Jin, Baobin Sun. (2012) CFD–DEM simulation of particle transport and deposition in pulmonary airway.

[18] X.Y. Luo, J.S. Hinton, T.T. Liew, K.K. Tan (2004). LES modelling of flow in a simple airway model.

[19] X.L. Yang, Yang Liu, H.Y. Luo. (2006). Respiratory flow in obstructed airways.

[20] Y. Liu, R.M.C. So, C.H. Zhang. (2002) Modeling the bifurcating flow in a human lung airway.

[21] Yasuo Sekine, Mehrdad Behnia, Takehiko Fujisawa.(2010) Impact of COPD on pulmonary complications and on long-term survival of patients undergoing surgery for NSCLC.

[22] Z. Zhanga, C. Kleinstreuer, C.S. Kimc (2001). Effects of curved inlet tubes on air flow and particle deposition in bifurcating lung models.

[23] Z. Zhanga, C. Kleinstreuer, C.S. Kimb (2002). Micro-particle transport and deposition in a human oral airway model.

[24] Z. Zhang, C. Kleinstreuer (2004). Airflow structures and nano-particle deposition in a human upper airway model.

[25] Weibel, E.R., 1963. Morphometry of the Human Lung. Springer,
Academic Press, Berlin, New York.

APPENDICE A1

Velocity Distribution of model 1

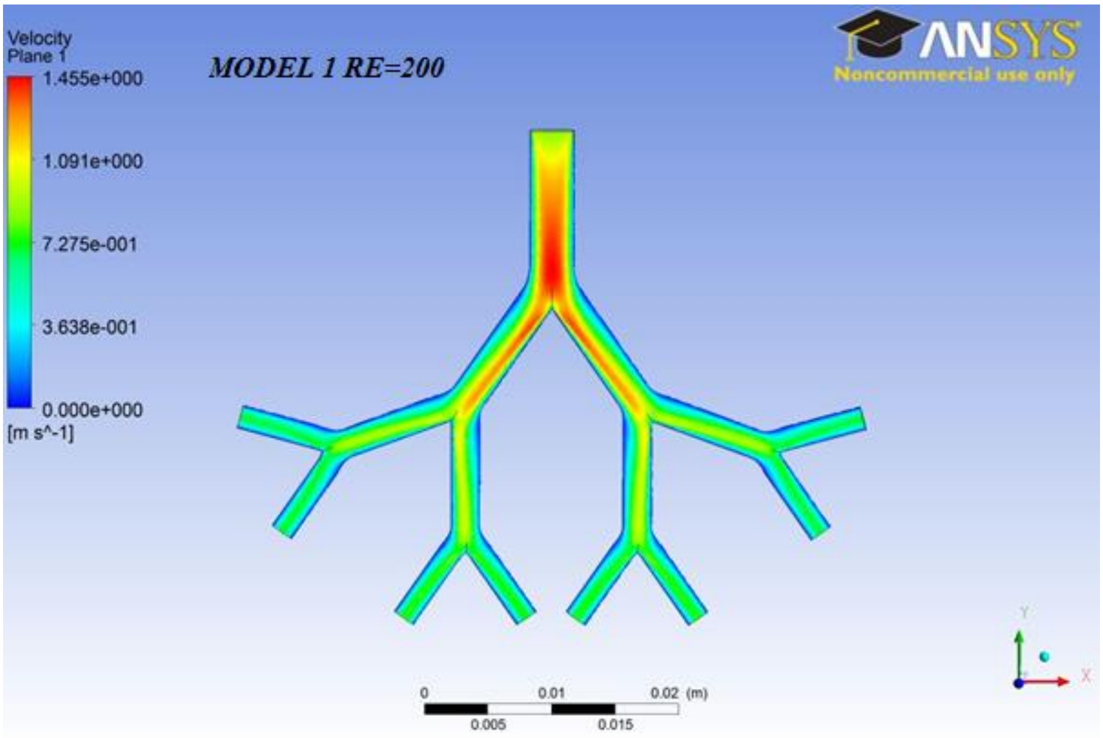

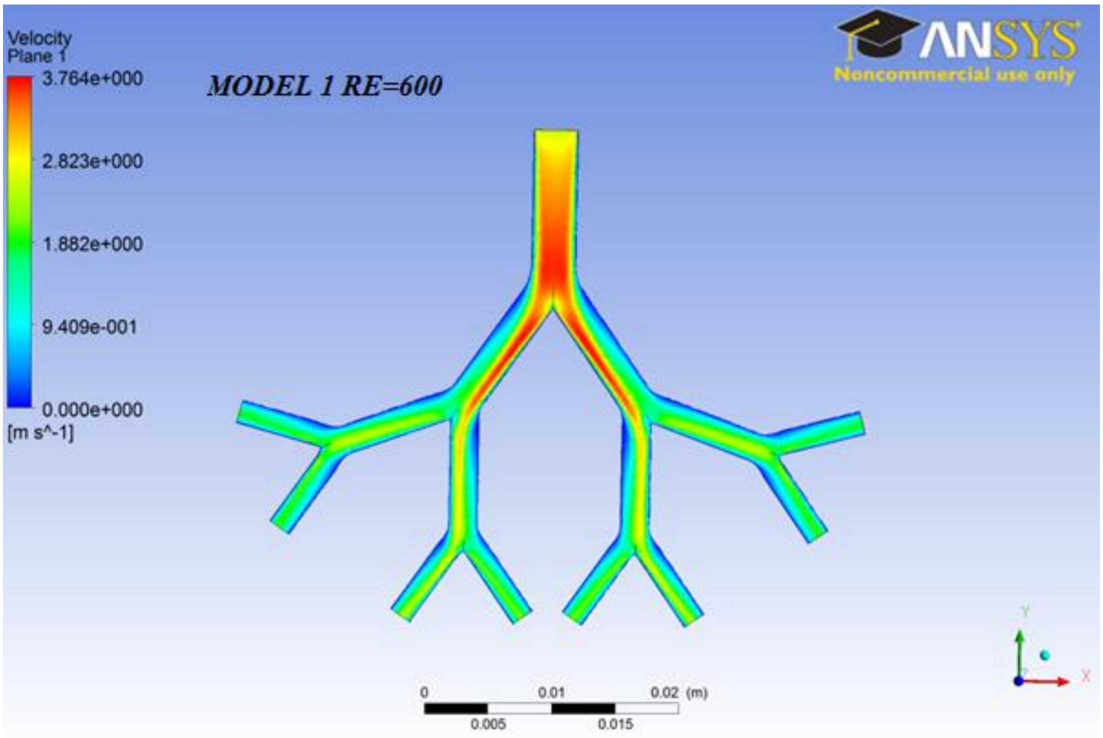

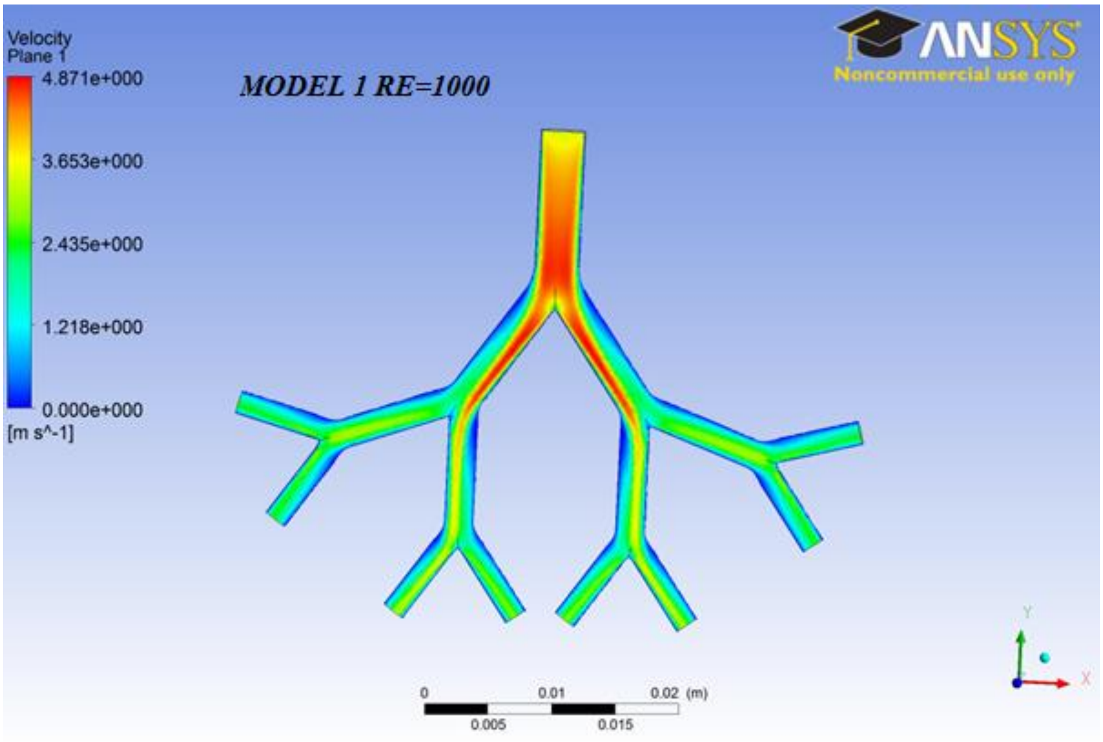
Velocity
Plane 1
4.871e+000
3.653e+000
2.435e+000
1.218e+000
0.000e+000
[m s^-1]
MODEL 1 RE=1000
ANSYS
Noncommercial use only
0
0.01
0.02 (m)
0.005
0.015
Y
X

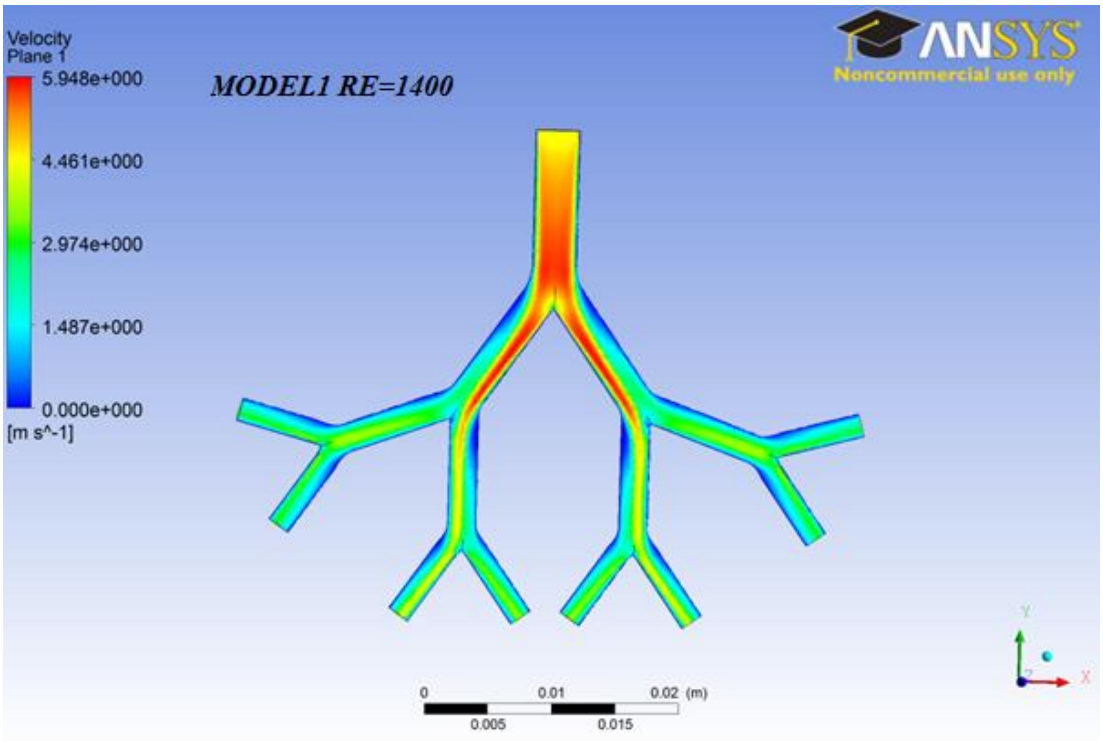
Velocity
Plane 1
5.948e+000
4.461e+000
2.974e+000
1.487e+000
0.000e+000
[m s^-1]
MODEL1 RE=1400
ANSYS
Noncommercial use only
0
0.01
0.02 (m)
0.005
0.015
Y
X

APPENDICE A2

Velocity Distribution of model 2

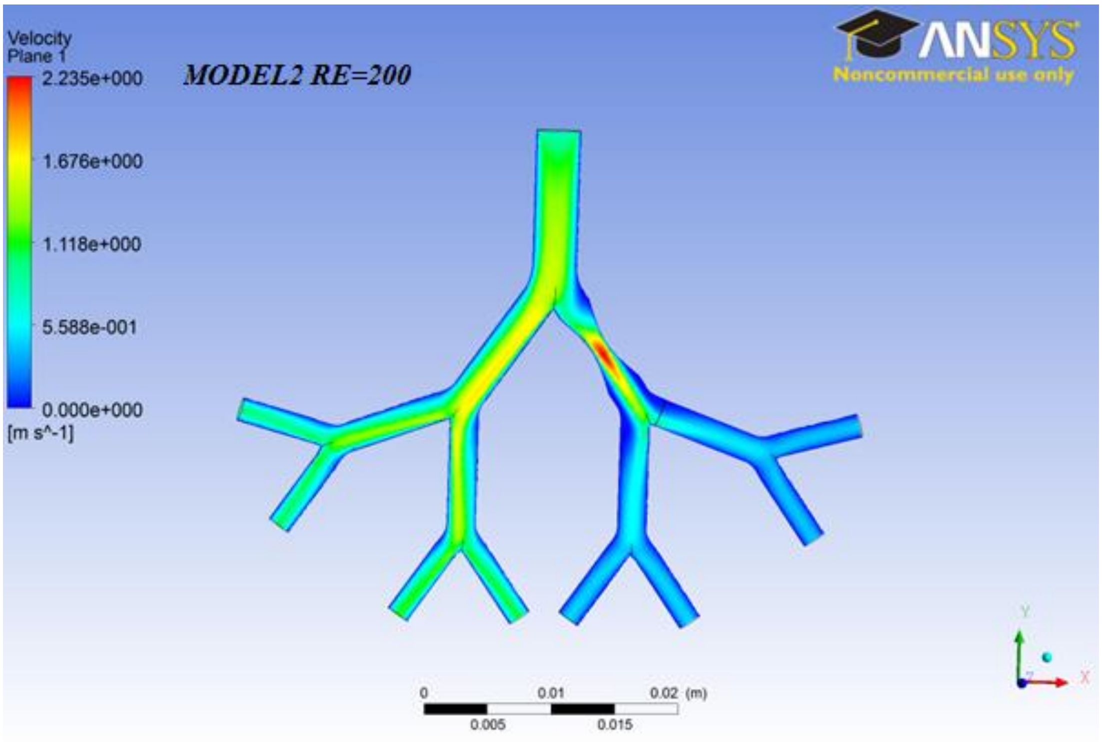

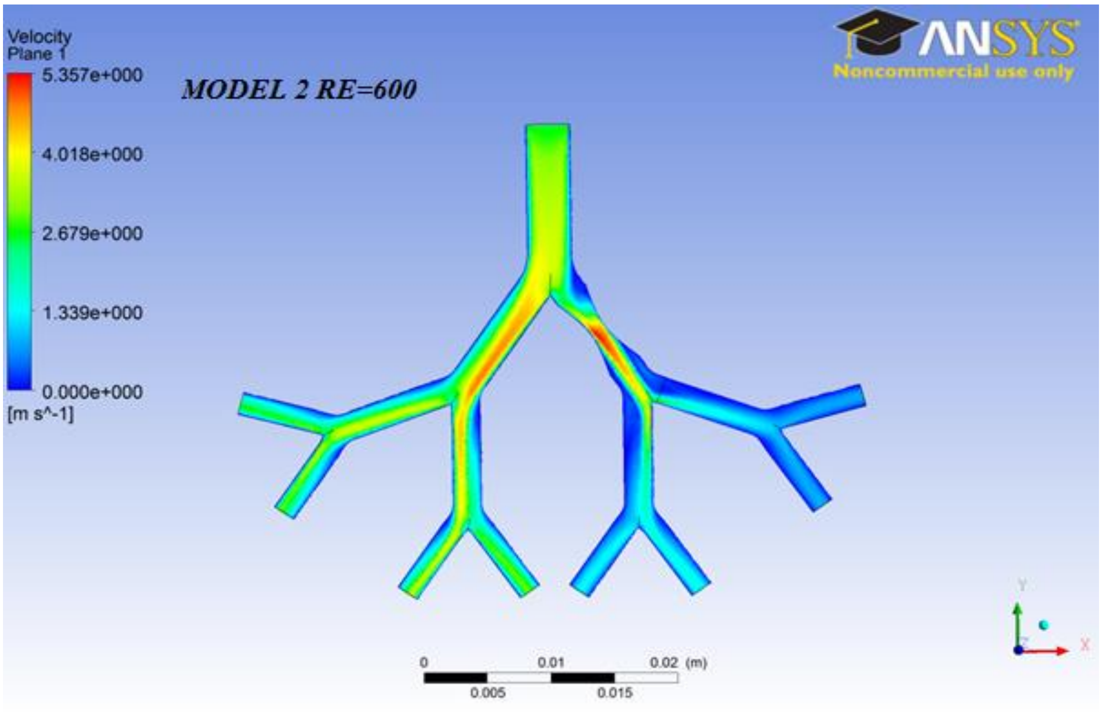

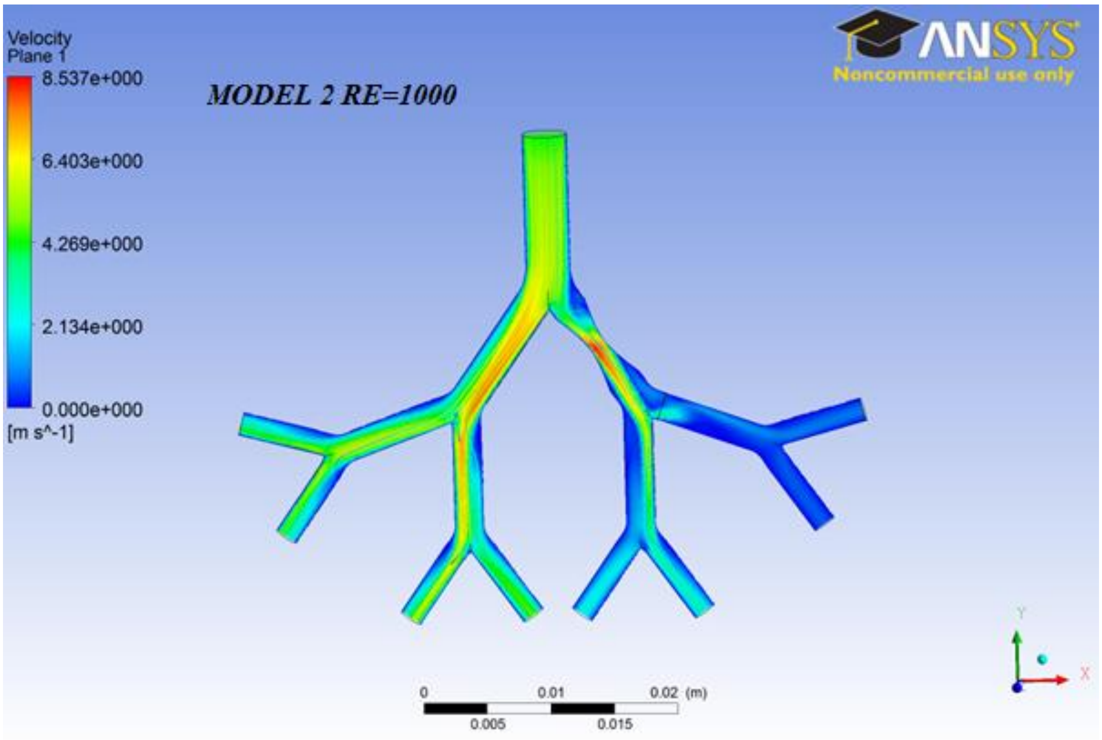
Velocity
Plane 1
8.537e+000
6.403e+000
4.269e+000
2.134e+000
0.000e+000
[m s^-1]
MODEL 2 RE=1000
ANSYS
Noncommercial use only
0
0.01
0.02 (m)
0.005
0.015
Y
X

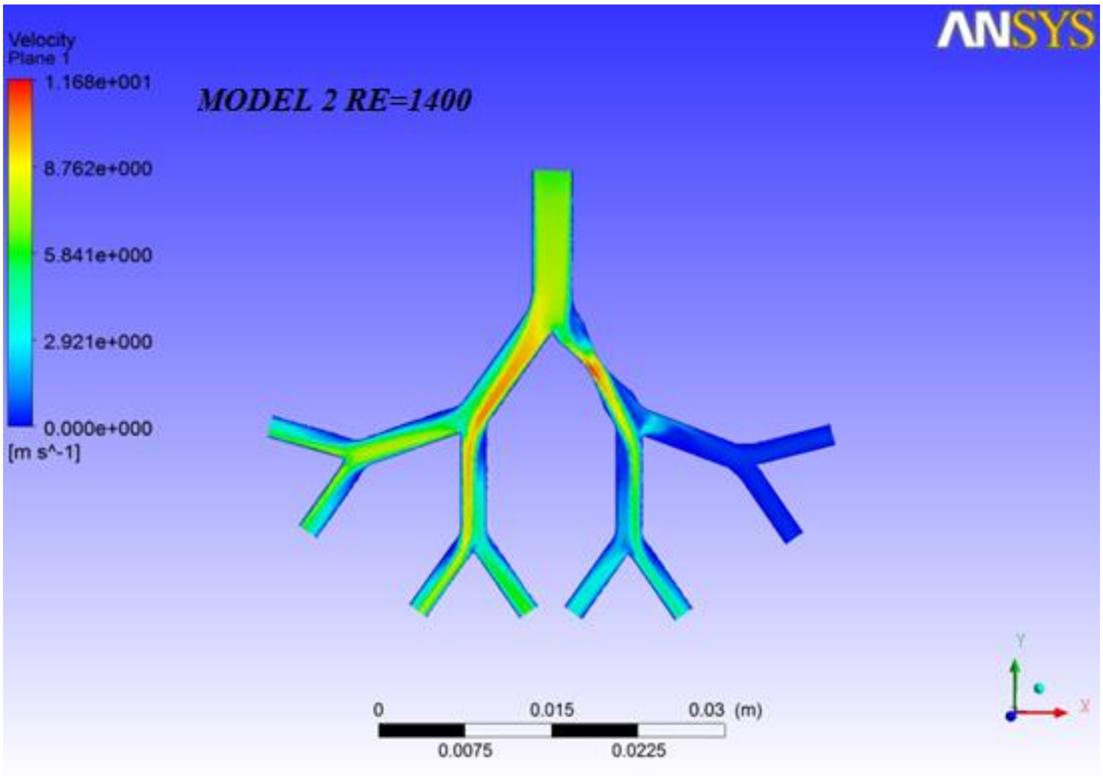
Velocity
Plane 1
1.168e+001
8.762e+000
5.841e+000
2.921e+000
0.000e+000
[m s^-1]
MODEL 2 RE=1400
ANSYS
0
0.015
0.03 (m)
0.0075
0.0225
Y
X

APPENDICE A3

Velocity Distribution of model 3

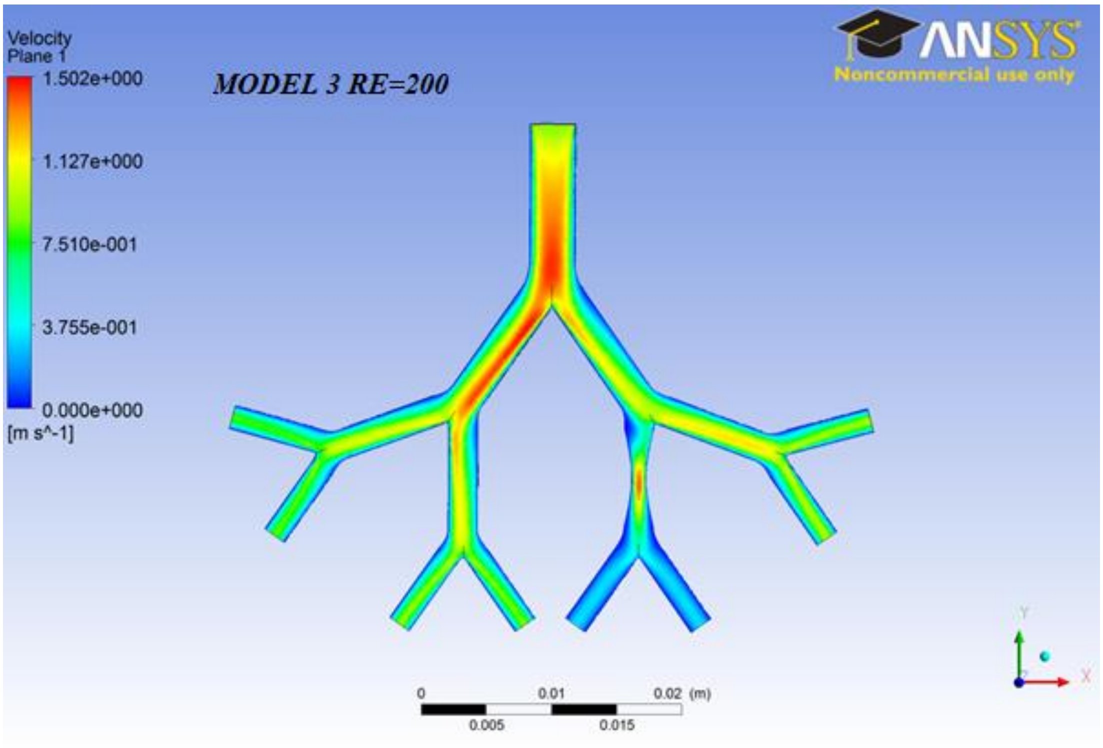

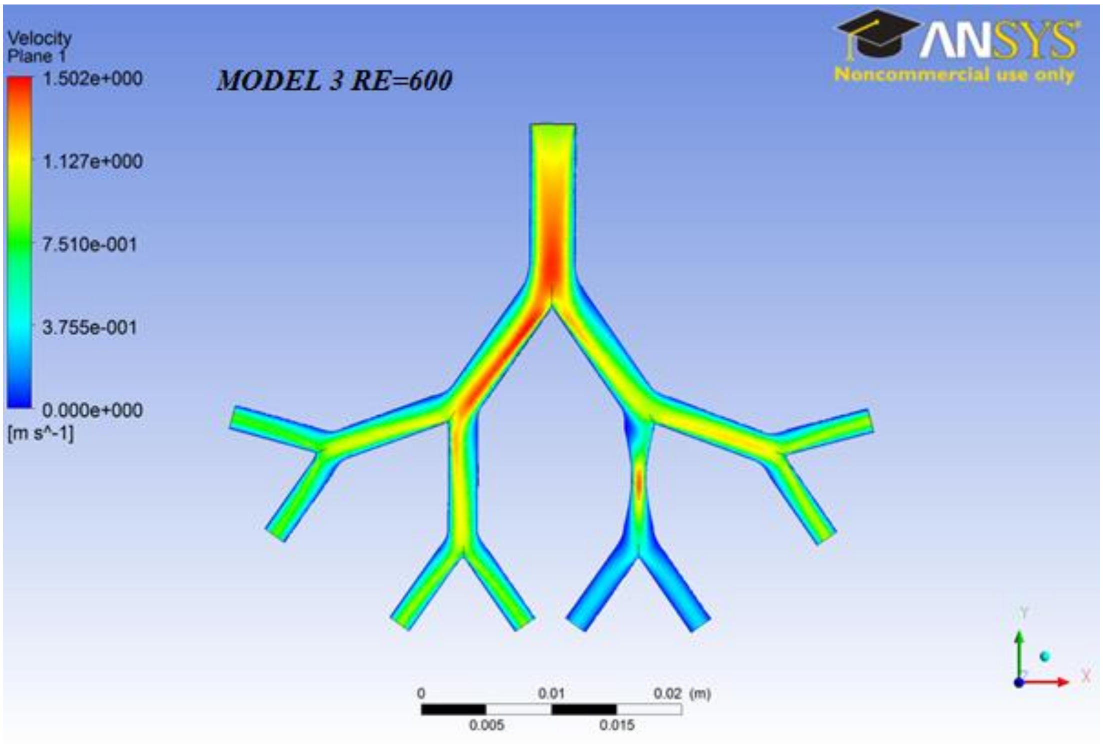

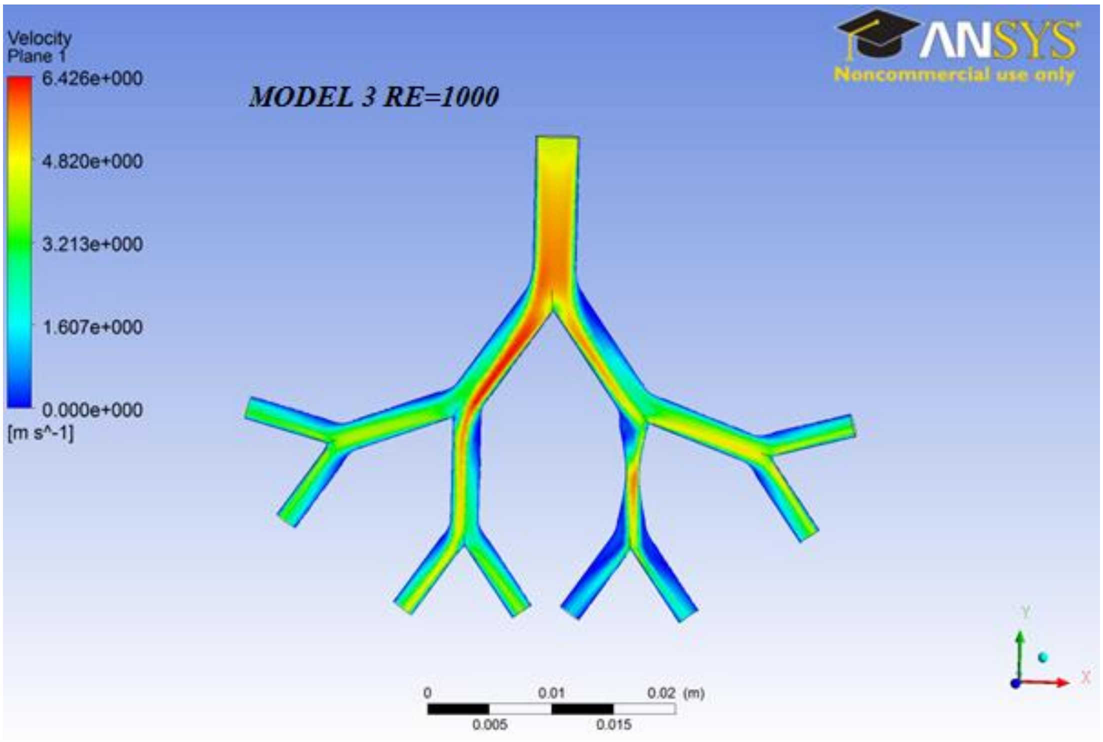
Velocity
Plane 1
6.426e+000
4.820e+000
3.213e+000
1.607e+000
0.000e+000
[m s^-1]
MODEL 3 RE=1000
ANSYS
Noncommercial use only
0
0.01
0.02 (m)
0.005
0.015
Y
X

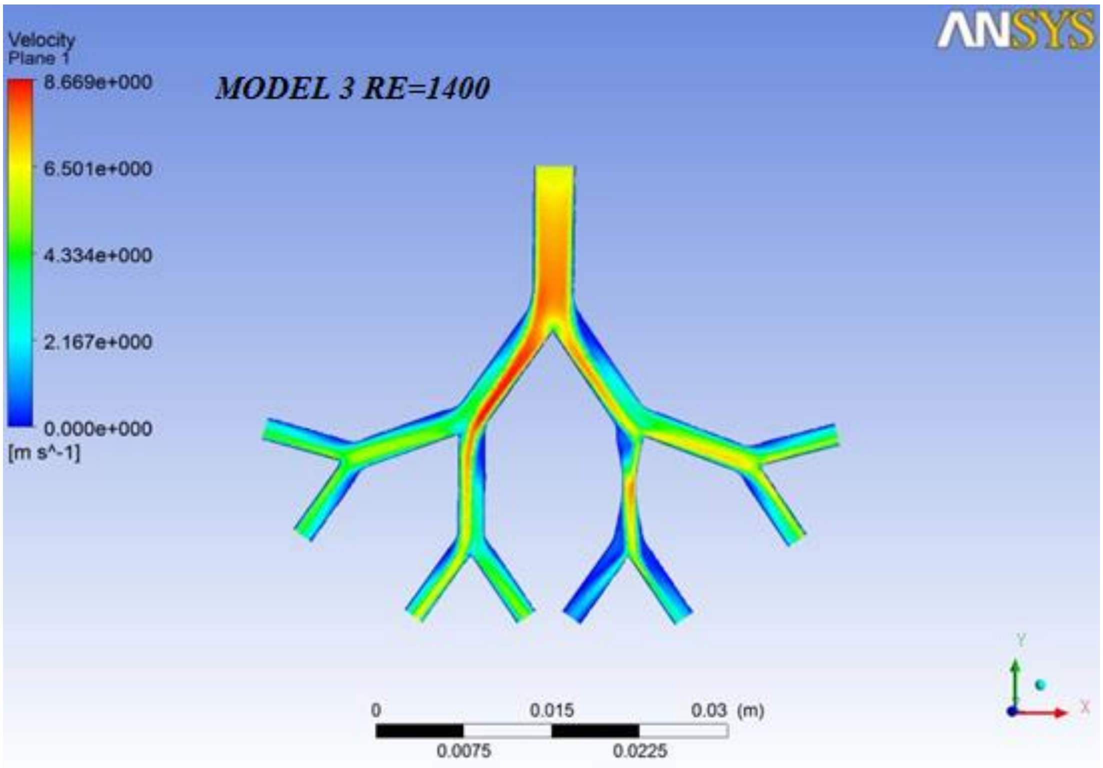
Velocity
Plane 1
8.669e+000
6.501e+000
4.334e+000
2.167e+000
0.000e+000
[m s^-1]
MODEL 3 RE=1400
ANSYS
0
0.015
0.03 (m)
0.0075
0.0225
Y
X

APPENDICE A4

Velocity Distribution of model 4

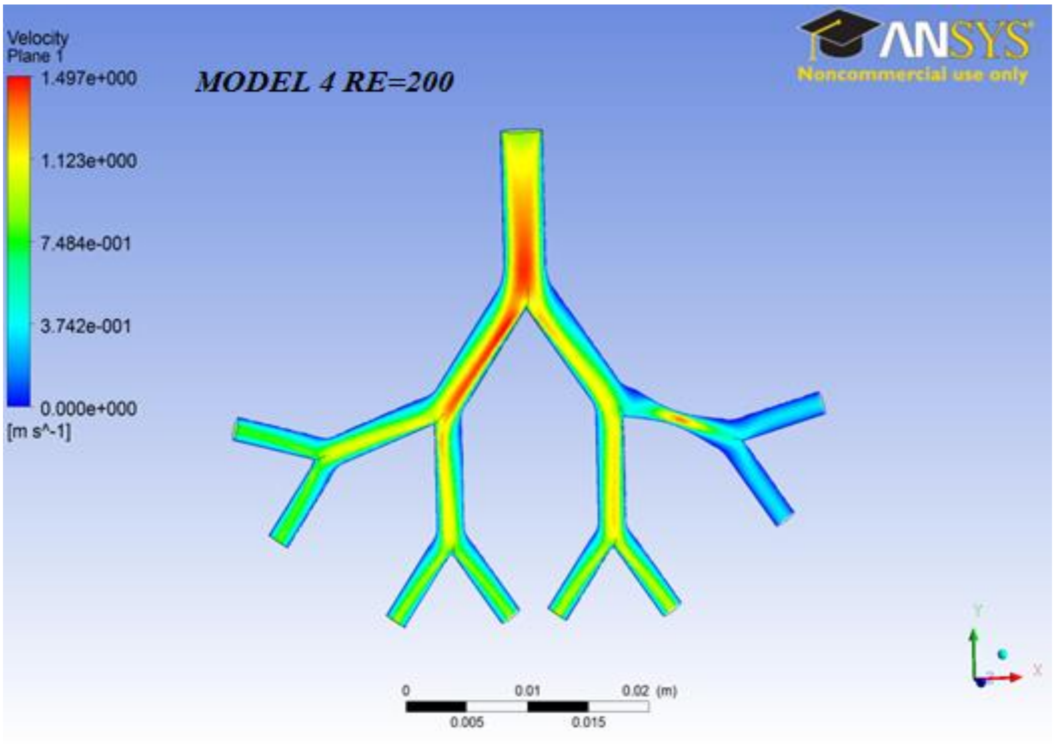

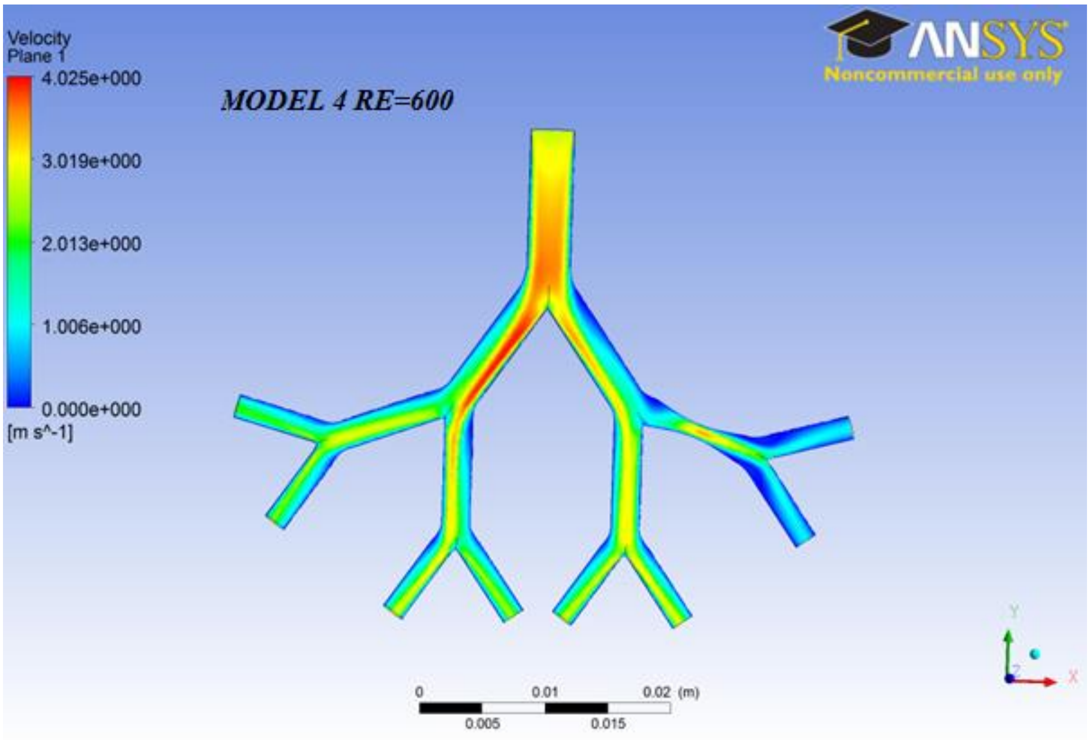

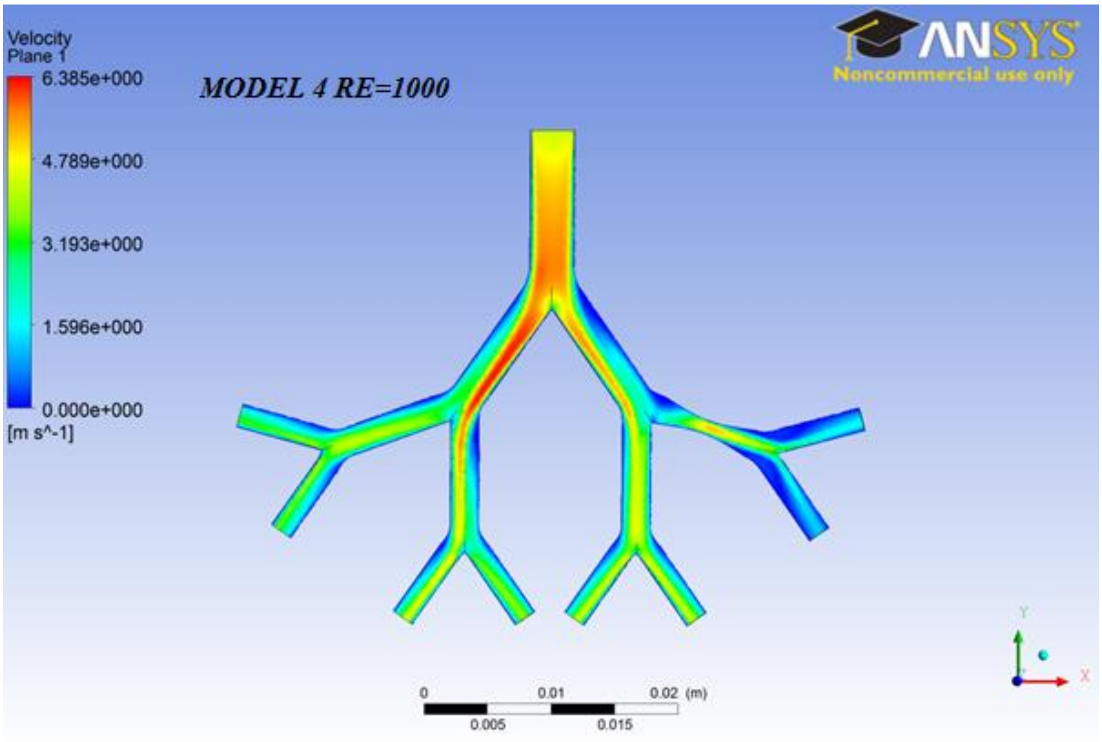
Velocity
Plane 1
6.385e+000
4.789e+000
3.193e+000
1.596e+000
0.000e+000
[m s^-1]
MODEL 4 RE=1000
ANSYS
Noncommercial use only
0
0.01
0.02 (m)
0.005
0.015

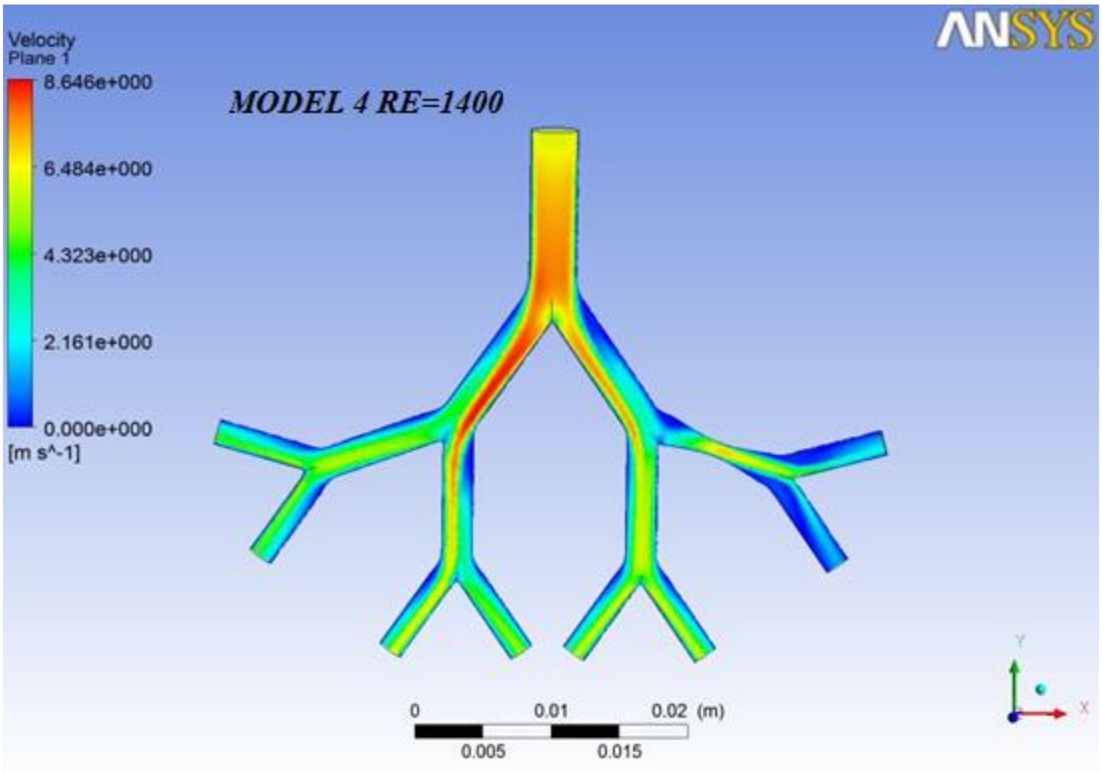
Velocity
Plane 1
8.646e+000
6.484e+000
4.323e+000
2.161e+000
0.000e+000
[m s^-1]
MODEL 4 RE=1400
ANSYS
0
0.01
0.02 (m)
0.005
0.015

APPENDICE A5

Air flow velocity at middle sections of a 4^{th} generation airway